

REDUCIBILITY PROPERTIES OF ERDEMIR SAMPLES

A THESIS SUBMITTED TO  
THE GRADUATE SCHOOL OF NATURAL AND APPLIED SCIENCES  
OF THE MIDDLE EAST TECHNICAL UNIVERSITY

BY

MURAT ÖZKAN AKSIT

IN PARTIAL FULFILLMENT OF THE REQUIREMENTS FOR THE  
DEGREE OF  
MASTER OF SCIENCE  
IN  
THE DEPARTMENT OF METALLURGICAL AND MATERIALS  
ENGINEERING

JANUARY 2004

## **ABSTRACT**

### **REDUCIBILITY PROPERTIES OF ERDEMIR SAMPLES**

Aksit, Murat Özkan

M.S., Department of Metallurgical and Materials Engineering

Supervisor: Prof.Dr. Yavuz Topkaya

January 2004, 107 pages

The effect of physical, chemical and mineralogical properties on reducibility of iron containing raw materials were studied with the use of two pellets, one sinter and one lump iron ore sample provided by Erdemir integrated iron and steel works. Although Erdemir lump iron ore contained hematite, it was found to be less reducible than Erdemir sinter since porous structures are easier to reduce and in general sinters have a higher porosity as compared to lump ores. Experimental findings indicated that Erdemir pellet with a code B had the highest reducibility. On the other hand, the results of Erdemir samples were compared with those results obtained from the projects carried out in the Metallurgical and Materials Engineering Department of METU in 1980's. In mentioned projects, samples of various lump iron ores and a concentrate, pellet and sinter from Turkish sources and imported lump iron ores of CVRD from Brazil and ISCOR from the Republic of South Africa were tested. Within the context of this thesis, a mathematical model that would fit to the reduction kinetics was studied and the porous solid model was found to be the best for Erdemir samples.

**Keywords:** Reducibility, RDI, pellet, sinter, lump ore, modeling

## ÖZ

### ERDEMİR NUMUNELERİNİN İNDİRGENME ÖZELLİKLERİ

Aksit, Murat Özkan

Yüksek Lisans, Metalurji ve Malzeme Mühendisliği Bölümü

Tez Yöneticisi: Prof.Dr. Yavuz Topkaya

Ocak 2004, 107 Sayfa

Demir içeren hammaddelerin fiziksel, kimyasal ve mineralojik özelliklerinin indirgenme özelliği üzerindeki etkilerinin belirlenmesi amacıyla sahip olan bu çalışmada Erdemir entegre demir ve çelik işletmesinden temin edilen sinter, cevher ve iki farklı pelet numunesi kullanılmıştır. Gözenekli numunelerin daha kolay indirgenebildiği; Erdemir cevherinin, içerdiği hematit mineraline rağmen Erdemir sinterinden daha az indirgenmesi ile belirlenmiştir. Bunun sinterlerin genelde parça cevherlere oranla daha gözenekli olmalarından kaynaklandığı düşünülmektedir. En yüksek indirgenme özelliğine sahip numune ise Erdemir B kodlu pelet olmuştur. Ayrıca Erdemir numunelerinin verileri, 1980'li yıllarda O.D.T.Ü. Metalurji ve Malzeme Mühendisliği Bölümünde yürütülen projelerde yer alan numunelerden elde edilen verilerle de karşılaştırılmıştır. Bu numuneler Türkiye'nin değişik bölgelerinden temin edilen parça cevherler ve konsantre, pelet ve sinter ile Brezilya'nın CVRD ve Güney Afrika Cumhuriyeti'nin ISCOR firmalarından ithal edilen parça demir cevherlerinden oluşmaktadır. Tez kapsamında ayrıca redüklenme kinetiğine uygun matematiksel modeller araştırılmış olup, Erdemir numunelerine gözenekli kati modelinin en uygun olduğu belirlenmiştir.

**Anahtar Kelimeler:** Indirgenebilirlik, RDI, pelet, sinter, parça cevher, modelleme

## **ACKNOWLEDGEMENTS**

I express sincere appreciation to Prof. Dr. Yavuz Topkaya for his continuous guidance and supervision throughout the course of this thesis study.

Thanks to Ibrahim am for X-ray analysis and related comments.

Erdemir Iron and Steel Works are greatly acknowledged for providing the lump iron ore, pellets and sinter and performing chemical analysis.

Technical support provided by Isa Hasar is greatly appreciated. I offer sincere thanks to Aydemir Gunaydin for his contribution and help.



2.4.1 Physical Strength .....	12
2.4.2 Reducibility .....	13
2.4.3 Reduction Disintegration .....	14
2.5 Sintering .....	15
2.5.1 Process Description .....	15
2.5.2 Sinter Mineralogy .....	16
2.5.3 Sinter Quality .....	18
2.5.3.1 Sinter Size Consist .....	18
2.5.3.2 Sinter Size Strength .....	18
2.5.3.3 Reducibility .....	19
2.5.3.4 Chemistry .....	20
2.6 Evaluation Properties of Burden Materials .....	20
2.6.1 Physical Properties of Burden Materials .....	20
2.6.2 Reducibility Tests .....	29
2.6.2.1 Gakushin Test .....	33
2.6.2.2 Verein Deutscher Eisenhüttenleute ( V.D.E. ) Method .....	36
2.6.2.3 Centre National de Recherches Metallurgiques ( C.N.R.M. ) Method ....	37
2.6.2.4 Non-Isothermal Test: Aufheizverfahren Method .....	37
2.6.2.5 Determination of Reducibility by I.S.O. 4695 .....	38
2.6.2.6 Iron Ores – Static Test for Low Temperature Reduction Disintegration ...	42
2.6.2.6.1 I.S.O. 4696-1: Reaction with CO, CO <sub>2</sub> and H <sub>2</sub> .....	42
2.6.2.6.2 I.S.O. 4696-2: Reaction with CO .....	46

2.6.2.7 I.S.O. 4697: Iron Ores Test Method for Low Temperature Disintegration – Tumbling during Reduction .....	49
2.6.2.8 Determination of Relative Reducibility by I.S.O. 7215 .....	52
2.6.2.9 I.S.O. 7992: Determination of Reduction Properties under Load .....	55
2.6.2.10 I.S.O. 13930: Dynamic Test for Low Temperature Reduction Disintegration ...	59
2.6.3 Correlation of Reducibility Indices .....	62
2.7 The Effect of Agglomeration on Blast Furnace Operation ..	63
3. EXPERIMENTAL .....	66
3.1 Experimental Set Up for the Reducibility and Reduction Disintegration ( RDI ) Tests .....	65
3.2 Preparation of the Test Samples .....	68
3.3 Measurement of True Density with Pycnometer .....	68
3.4 Measurement of Apparent Density with Pycnometer .....	70
3.5 Reducibility Test .....	72
3.6 Reduction-Disintegration Test .....	73
4. RESULTS and DISCUSSIONS .....	75
4.1 Mineralogical Structures and Chemical Compositions of Erdemir Samples .....	75
4.2 Results of Apparent and True Density Measurements .....	76
4.3 The Results of Reduction-Disintegration Tests .....	79
4.4 The Results of Reducibility Tests of Erdemir Samples .....	81
4.5 Evaluation of the Reducibility and Other Test Results .....	88
4.6 Models for Reduction .....	95
4.6.1 Retracting Core Model .....	95
4.6.2 Porous Solid Model .....	97
5. CONCLUSIONS .....	101
REFERENCES .....	103



## LIST OF TABLES

### TABLE

2.1 Mineralogy of Iron Ore .....	8
2.2 Tumbling and Abrasion Tests .....	24
2.3 Typical Linder Test Results .....	32
2.4 Various Versions of the Gakushin Method of Reducibility Testing .....	33
2.5 Chiba Test – Reducibility Index Results .....	35
4.1 Mineralogical Structures of Erdemir Samples and the Others .....	75
4.2 Chemical Compositions of Erdemir Samples .....	76
4.3 True Density, Apparent Density and Total Porosity Values of Erdemir Samples and the Others .....	78
4.4 RDI Values of Erdemir Samples and the Others .....	80
4.5 Reducibility Values of Erdemir Samples and the Others at the End of Three Hours .....	85
4.6 Reducibility Indices of Erdemir Samples and the Others ....	98

## LIST OF FIGURES

### FIGURE

2.1 Relative Reducibility of Blast Furnace Feeds .....	14
2.2 Linder Reduction Test Apparatus .....	30
2.3 Gakushin Reduction Test Apparatus .....	34
2.4 Aufheizverfahren Apparatus .....	38
2.5 Arrangement of a Test Unit for Determination of Reducibility According to I.S.O. 4695 .....	40
2.6 Arrangement of a Test Unit for I.S.O. 4696 .....	44
2.7 Example of Tumbler Drum for I.S.O. 4696-2 .....	48
2.8 Arrangement of Reduction Apparatus for I.S.O. 4697 .....	50
2.9 Schematic Diagram of Reduction Test Apparatus for I.S.O. 7215 .....	53
2.10 Apparatus for Determining Reduction Properties under Load for I.S.O. 7992 .....	57
2.11 Low Temperature Disintegration Test Apparatus for I.S.O. 13930 .....	60
3.1 Set up for the Reduction and Reduction Disintegration Tests .....	66
3.2 Experimental Set up Showing the Electrically Heated Furnace and Test Tubes used in the Reduction and Reduction Disintegration Tests .....	67
3.3 Drawing of the Mercury Pycnometer .....	72
3.4 Drawing of the Tumbler Drum used in Reduction Disintegration Test .....	74
4.1 Results of the Reduction Disintegration Tests of Erdemir Samples .....	81

4.2 Reducibility Curve of Erdemir Sinter .....	86
4.3 Reducibility Curve of Erdemir Pellet A .....	86
4.4 Reducibility Curve of Erdemir Pellet B .....	87
4.5 Reducibility Curve of Erdemir Lump Ore .....	87
4.6 Comparison of Reducibilities of Erdemir Samples .....	88
4.7 Comparison of Reducibilities of Lump Ores .....	90
4.8 Comparison of Reducibilities of Pellets .....	91
4.9 Comparison of Reducibilities of Sinters .....	92
4.10 $[-\ln(1-R\% / 100)]$ vs Time ( t ) Graph to Determine the Reducibility Index for Erdemir Sinter .....	99
4.11 $[-\ln(1-R\% / 100)]$ vs Time ( t ) Graph to Determine the Reducibility Index for Erdemir Pellet A .....	99
4.12 $[-\ln(1-R\% / 100)]$ vs Time ( t ) Graph to Determine the Reducibility Index for Erdemir Pellet B .....	100
4.13 $[-\ln(1-R\% / 100)]$ vs Time ( t ) Graph to Determine the Reducibility Index for Erdemir Lump Ore .....	100

## **CHAPTER 1**

### **INTRODUCTION**

In modern blast furnace operation, careful burden preparation to provide a rigorously sized burden of consistent chemical analysis is essential in order to obtain high furnace productivity. Intensive work into the improvement of burden preparation and quality has identified facets of burden properties which can play an important part in furnace operation.

As it is becoming increasingly important to know the physical and chemical properties of the individual burden constituents, many test procedures have been and are being developed to determine and quantify various properties.

In considering the performance of the materials inside the furnace under reducing conditions, it is accepted that it is difficult to develop tests which can precisely simulate furnace conditions. Many tests have been developed in an endeavor to obtain meaningful information which is of assistance to blast furnace operators. As the blast furnace is final smelter of any material, it is important to carry out blast furnace trials to evaluate a specific material under test conditions, in order to correlate the results with laboratory tests. Various practices in furnace operation and local economics must be borne in mind attempting to determine the acceptable level of any specific property of a burden.

An important characteristic of a burden material is its reducibility, e.g., the ease with which oxygen can be removed. Reducibility data give an indication of the fuel required in the blast furnace and also provide information for determining the

optimum size range in which any material should be employed. The ideal method of determining reducibility of iron-bearing materials should use the same size grading as that charged to the furnace using gas flow rates, temperatures, and gas compositions, varying in a manner simulating that in the blast furnace. This, however, is difficult to effect for a routine method, as the apparatus becomes sophisticated and the procedure complicated, and several skilled operators are required [1].

The reducibility test method is one of the several procedures used to evaluate the behavior of natural and processed iron ores and agglomerates such as sinters and pellets under specific conditions.

The aim of this thesis was to test four different samples supplied by Erdemir Iron and Steel Works. The samples consisted of two different kinds of imported pellets, one lump iron ore and the representative sample of sinter used at Erdemir in the year 2001. After the physical, chemical and mineralogical characterization of the samples, they were subjected to reducibility tests and the results obtained were compared with those obtained for other local and imported ores, Divrigi pellet and Kardemir sinter.

## CHAPTER 2

### LITERATURE SURVEY

#### 2.1 Nature of Iron Ore

Iron is only found in metallic state in certain types of meteorites but, in a combined form, it is one of the most common elements, comprising some 5 % of the earth's crust. It is most usually found as an oxide, sometimes a hydrated oxide, but it also occurs as carbonate and sulphide and as a component of a wide range of complex minerals.

An iron-bearing mineral can only be considered to be an iron ore if the total cost of extracting iron from it is comparable with the cost of extracting iron from other ores. This will be governed by many factors, of which the iron content of the mineral, the nature of the impurities and the location of the deposit are of particular importance [2].

The more economically important iron-bearing minerals are the following:

Hematite	$\text{Fe}_2\text{O}_3$
Magnetite	$\text{Fe}_3\text{O}_4$
Limonite, goethite and hydrogoethite	Hydrated hematites
Siderite	$\text{FeCO}_3$
Chamosite	$3\text{FeO} \cdot \text{Al}_2\text{O}_3 \cdot 2\text{SiO}_2 \cdot 3\text{H}_2\text{O}$

In addition, iron is recovered from a number of minerals from which other saleable products are also extracted: for example, from pyrites ( $\text{FeS}_2$ ) and pyrrhotite ( $\text{FeS}$ ), in addition to sulphur; from ilmenite ( $\text{FeTiO}_3$ ), in addition to titania, and from complex ores, in addition to such metals as nickel, copper, cobalt and vanadium.

### **2.1.1 Hematite**

Hematite is widely distributed and is the most important source of iron. When pure, it contains 70 % of iron. Much of the hematite mined is high-grade, with 64-68 % iron and only small quantities of impurity, mainly silica and alumina. The sulphur and phosphorus contents are normally very low. There are also very large deposits of low-grade hematite containing only 20-40 % iron with high silica contents, some of which are now being mined. Much of the silica is removed by mineral dressing and a product is obtained which contains 60-70 % of iron.

### **2.1.2 Magnetite**

Deposites of high grade magnetites occur in a number of places, the best known being in Sweden. When pure, magnetite contains 72.4 % iron, the high grade ore contains more than 60 % iron with phosphorus-containing minerals, e.g., apatite, as a common impurity. Low grade magnetite deposits are also worked in many places, and a product is obtained after mineral dressing which has an iron content in excess of 60 %.

### **2.1.3 Limonite, Goethite, Hydrogoethite**

These are all hydrated iron oxides containing, when pure, 60-63 % iron. On heating, the water molecules are removed. They can occur as primary minerals or may be produced relatively near the surface as a result of weathering of the exposed ore. In low-grade silicate deposits, weathered outcrops of hydrated ore

occur in which the iron content is greatly enriched. Such outcrops provided ore for the first steel industries.

#### **2.1.4 Siderite**

This mineral constitutes only a small proportion of the total world iron ore reserves. When pure, it contains 48 % iron, but it is easily decomposed by heat (calcined) to hematite with 70 % iron. Siderite is still a commercially important source of ore in some countries, e.g, Canada.

#### **2.1.5 Chamosite**

This mineral occurs, together with limonite and siderite, in relatively low grade. "Minette" type deposits, such as those of France (Lorraine) and the United Kingdom. In these countries it is important source of iron. These ores usually contain some sulphur and phosphorus and such minerals as quartz and calcite.

#### **2.1.6 Impurities**

All iron ores contain impurities, which are collectively known as gangue. The complex mineral chamosite can be regarded as a mixture of iron oxide (FeO) and gangue ( $\text{SiO}_2$  and  $\text{Al}_2\text{O}_3$ ). These impurities may be divided into the following categories.

##### **2.1.6.1 Slag Forming**

These are, in the main, four oxides namely silica ( $\text{SiO}_2$ ) and alumina ( $\text{Al}_2\text{O}_3$ ) which are acidic and lime (CaO) and magnesia (MgO) which are basic. Of these oxides, only  $\text{SiO}_2$  can be reduced during ironmaking and usually only to a very limited extent. In conventional ironmaking by the blast furnace process, a liquid slag is formed in which the ratio by weight of bases (CaO + MgO) to acids ( $\text{SiO}_2 + \text{Al}_2\text{O}_3$ ), called the basicity, is normally about one. Most ores have an



excess of  $\text{SiO}_2$  and  $\text{Al}_2\text{O}_3$  and the ash of the coke used for fuel is mainly composed of these oxides, so a basic flux, e.g., limestone, must be added.

In certain regions, in particular where “Minette” type ores are used, it is possible to mix ores with a predominantly acid gangue with those whose gangue is basic to obtain a “self-fluxing” ore mix, and so to avoid the use of limestone.

#### **2.1.6.2 Metallic Oxide which are Largely Reduced to Metal during Ironmaking**

Manganese oxides are the most common, other oxides are those of chromium and nickel. Some metal oxides, e.g., nickel, are more easily reduced so that a major proportion of them go to the metal, the remainder going, as oxide, to the slag. A manganese content of around 1 % is advantageous but small proportions of other metals, e.g., chromium, are undesirable. The large deposits of lateritic ores, which consist predominantly of hydrated oxides, contain appreciable quantities of chromium, nickel and cobalt. In some areas, e.g., West Africa, they have been extracted and sold for their iron content, whilst in others they are worked for their non-ferrous metal content, e.g., nickel in New Caledonia.

#### **2.1.6.3 Deleterious Impurities**

Both sulphur and phosphorus impart undesirable properties to steel and must be kept below certain maximum levels. Sulphur can be reduced to the desired level during ironmaking but an increased sulphur intake increases the cost of ironmaking. Normally, some ores have a relatively high sulphur content. These can be given some pretreatment to reduce the sulphur level; when iron is extracted from pyrite and pyrrhotite the sulphur is first removed by roasting, the ore being converted to an oxide. Phosphorus can not be removed during ironmaking but this can, if necessary, be done when the iron is refined to steel. However, the most economic modern steelmaking process, basic oxygen steelmaking, is mainly used if the phosphorus content of the iron is low. This means that low phosphorus ores,

with a phosphorus/iron weight ratio of 0.002 or less, are preferred. Other deleterious impurities are the alkalis ( $\text{Na}_2\text{O}$ ,  $\text{K}_2\text{O}$ ) and  $\text{TiO}_2$ .

## **2.2 Iron Ore, Iron Minerals and Ore Mineralogy**

Iron is one of the most abundant elements in the earth, constituting about 5 % of the earth's crust [3]. Almost all rocks, with the exception of a few limestones, contain some iron, but iron deposits are usually limited to those containing 25 to 70 % iron or roughly 5 to 15 times the average iron content of the earth's crust.

All iron ore deposits contain one or more iron-rich minerals and the physical and chemical properties of any specific ore are related to the mineralogy of the deposit. Today, in beneficiation and agglomeration plants, the mineralogy is often more important than the grade of the crude ore, as the concentration and indurations properties are dependent upon the minerals present and on their physical relationship in the ore.

There are many iron-bearing minerals. The most common ones are magnetite, hematite (including martite), goethite, limonite, siderite and pyrite.

The most important iron ore minerals can be grouped according to their chemical composition into oxides, hydrous oxides, carbonates, sulphides, and iron silicates (see Table 2.1). The great bulk of iron ore consists of the first two groups which are oxides and hydrous oxides. Iron carbonates and sulphides are local sources of iron and, although mined for their iron content, are usually converted to oxides by calcining and roasting before being sent to the blast furnaces.

Table 2.1 Mineralogy of Iron Ore

Iron Ore Minerals	Chemical Composition	%Iron	Specific Gravity	Hardness	Crystallization	Color	Notes and Distinguishing Characteristics
<i>Oxides</i>							
Magnetite	Fe <sub>3</sub> O <sub>4</sub>	72.4	4.5-5.3	5.5-6.5	Isometric Octahedrons	Black	Strongly magnetic
Hematite	Fe <sub>2</sub> O <sub>3</sub>	69.94	5.2	5 to 6	Hexagonal Rhombohedral	Red to steely blue and brownish black	Red streak, non-magnetic
Martite	Fe <sub>2</sub> O <sub>3</sub>	70	4.8-5.3	6 to 7	Octahedrons	Black	Pseudomorphic after magnetite
Maghemite	Fe <sub>2</sub> O <sub>3</sub>	69		5	Isometric Massive	Brown	Highly magnetic
Ilmenite	FeTiO <sub>3</sub>	36.8-Fe 31.6-Ti	4.7	5.5-6.7	Hexagonal Rhombic	Iron black to brownish black	Slightly magnetic
<i>Hydrous Oxides</i>							
Goethite	FeO(OH)	62.9	4.3	5 to 5.5	Orthorhombic	Yellowish brown to dark brown	
Lepidocrocite	FeO(OH)	62.9	4	5	Orthorhombic	Rudy red to reddish brown	Streak dull orange
Limonite	FeO(OH)nH <sub>2</sub> O	Variable 52.3-66.3	2.7-4.3	Variable 4 to 5-1/2		Various shades of brown and yellow	A field term for hydrous iron oxides of uncertain species
Turgite	2Fe <sub>2</sub> O <sub>3</sub> .H <sub>2</sub> O (variable H <sub>2</sub> O)	40-50	4.2-4.7	2 to 4	Amorphous	Reddish black to dark red	Not a mineral species. in part a metacolloid
<i>Carbonates</i>							
Siderite	FeCO <sub>3</sub>	43.2	3.8		Rhombic	Light to dark brown	
<i>Sulphides</i>							
Pyrite	FeS <sub>2</sub>	46.6	5	5 to 6.5	Isometric	Brass yellow	
Pyrrhotite	Fe <sub>1-x</sub> S	57-63.5	4.6	3.5-4.5	Hexagonal	Bronze yellow	Magnetic

## 2.3 Commercial Classification, Types and Specifications of Iron Ores

The important technical factors that determine the usability and thus the value of iron deposits are;

- 1) Its iron content
- 2) Its chemical composition other than iron
- 3) Its physical characteristics
- 4) Its amenability to concentration

### 2.3.1 Chemical Considerations of Iron Ores

The chemical composition of an ore is determined by its mineralogy; ore made up of different minerals of necessity have quite different chemical analysis. An ore consisting of pure siderite ( $\text{FeCO}_3$ ), for example, could not contain over 48 % iron, whereas an ore consisting of pure magnetite could contain slightly more than 72 %. A limonite-goethite ( $\text{Fe}_2\text{O}_3 \cdot x\text{H}_2\text{O}$ ) ore containing 62 to 63 % iron would contain less than 2% of slag forming components, but would have an ignition loss of close to 10 %. A hematite ore with the same iron analysis would have no ignition loss, but would contain a total of 8 to 10 % slag forming materials.

Impurities are present in all iron ores and important cost factors in both concentrating and pelletizing plants and in the blast furnace. If they are not removed by the concentration process, they must be transported and processed in the blast furnace, entailing additional costs for coke and fluxstone in the blast furnace. In addition to increasing costs, some impurities are objectionable in the furnace operation while others affect the quality of the pig iron.

In general, impurities in direct shipping ores, concentrates and agglomerates may be classed as “enhancing” or as “deleterious”. Enhancing impurities include any material present which aids the blast furnace processing or adds value to the hot metal produced. These materials include manganese minerals and the fluxes such

as lime, magnesia, and fluorspar. Deleterious impurities have adverse effect on furnace operation, hot metal quality and the fluidity of the slag. Certain impurities such as titanium and sulphur, even when present in small amounts, may significantly decrease the value of an ore with high iron content.

In addition to the consideration of impurities, there are several other chemical factors;

- 1) Moisture: Moisture is an important factor in the evaluation of iron ore not only because it adds to the weight of ore to be handled, but also because iron ore mining and ore sales are based on “natural” analyses in which the free water contained in the ore is considered as part of the overall chemical analysis.

Free moisture should not be confused with loss on ignition (L.O.I.).

- 2) Basicity: The basicity provides a means to calculate the amount of limestone, or other flux, to be added to the blast furnace burden to produce of a slag of the proper composition and consistency and to facilitate the smelting of the ingredients of the burden. The basicity of an ore may be calculated in one of two ways;

- a)  $(\text{wt\% CaO} + \text{wt\% MgO}) / \text{wt\% SiO}_2$  (ideally – 1.4)

- b)  $(\text{wt\% CaO} + \text{wt\% MgO}) / (\text{wt\% SiO}_2 + \text{wt\% Al}_2\text{O}_3)$  (ideally – 1.0 to 1.1)

- 3) Iron - Silica Ratio: The iron-silica ratio and the iron-acid ratio (sometimes expressed as the Rice Ratio),  $\text{Iron} / (\text{Silica} + \text{Alumina})$ , together with the basicity of the ore, determine the total amount of slag which will be produced from any given ferrous burden material when smelted in the blast furnace. The optimum ratio for each furnace is that which gives the minimum slag volume.

- 4) Reducibility: The reducibility is a measure of the ease with which the iron oxide in the direct shipping or beneficiated product are reduced, or deoxidized, to metallic iron in the blast furnace. In general, the greater the ease of the reduction, the more desirable the material is as a furnace burden. Degradation during reduction, however, is also an important consideration. Reducibility is a function of the constituents' minerals and the size and the porosity of individual particles. The relative reducibilities of minerals and agglomerates are: (a) limonite and goethite, (b) hematite, (c) pellets, (d) sinter and (e) magnetite. Natural magnetites are the most difficult to reduce.

### **2.3.2 Physical Considerations of Iron Ores**

Physical characteristics of concern are:

- 1) Durability: An ideal ore or beneficiated product should be abrasion resistant and strong enough to be handled and transported without creating excessive "fines"; it should be able to tolerate the stresses which occur in the column of ferrous burden, coke and fluxstone in a blast furnace without undue crushing. Magnetite ores are usually strong and dense. Hematite, goethite and limonite ores range from strong, dense varieties to those which are soft or earthy and, therefore, weak. Carbonate ores range from strong to soft. Fresh taconites and jaspilites are generally strong and dense, whereas their oxidized or decomposed equivalents are usually soft and weak.
- 2) Bulk Density, Porosity and Permeability: The bulk density of a direct shipping ore or a beneficiated product depends upon its mineral content, the internal porosity of the individual pieces and the size distribution. The permeability of the burden material affects the amount of wind which can

be blown into furnace; the porosity of individual particles influences the reducibility.

- 3) Ore Structure: Often referred to as screen analysis or size consist or size distribution. This property is usually measured by determining the percentages of material retained between consecutive screens or mesh size.

## **2.4 Pelletizing**

### **2.4.1 Physical Strength**

Pellets should have sufficient structural strength to withstand, without significant breakage, the normal handling which occurs during transportation and handling steps between the pellet furnace and the blast furnace skip.

A standard tumbling test was developed some years ago by the A.S.T.M. for evaluating the quality of coke, and most pellet producers use some form of this procedure.

A representative sample of pellets is dry-screened by hand at 3 meshes. The weight of each fraction is recorded. Any fused clusters are removed from the +3 mesh fraction and a 25 lb sample is riffled out, poured into the tumble drum, and allowed to tumble for 200 revolutions at a speed of 24 rpm. The tumbled material is hand screened on 3 meshes. Any loss in weight is assumed to be in the -3 mesh fraction. The +3 mesh fraction is reported as the "Tumble Index". The steel tumble drum is 3 ft in inside diameter by 18 inches long and is equipped with 2 internal lifters each 2 inches wide.

When comparing the quality of products from different plants, it is necessary to know the limiting screen on which the tumble index is based. Most good production pellets today will have 95 % or more plus 3 mesh following tumble testing.

Another method which is common use for evaluating the strength of pellets is the compression test. A representative number of pellets, usually 100, between 7/16 inches and 1/2 inches in diameter are broken in compression. Pellets of commercial quality will usually average a compression strength of between 300 lbs and 800 lbs. Laboratory pellets in this size range may have a compression strength well over 1000 lbs. Compression tests are best used to determine the uniformity of firing. A wide spread in compressive strength values will indicate lack of homogeneity in the product. If a pellet of the size range mentioned has a compression strength of under 200 lbs, it probably will not survive transportation and handling without breakage.

#### **2.4.2 Reducibility**

Because of their high microporosity, pellets usually reduce considerably faster than hard-burdened sinter or hard natural ores as shown in the Figure 2.1. In the earlier days of pelletizing, considerable weight was given to means of securing a high porosity for high reducibility. It became evident, however, than an easily reduced pellet was of little use if its strength was such that it was likely to disintegrate before reaching the furnace. The emphasis of late years has therefore been first on strength then on reducibility. Self fluxed pellets usually reduce at a somewhat slower rate than those in which the bond is chiefly by grain growth bridging. The presence of slag as a bonding constituent tends to cause shrinkage of the pellets and reduce the microporosity which, in turn, increases the time required for reduction. These effects are brought out by Merklin and De Vaney [4].



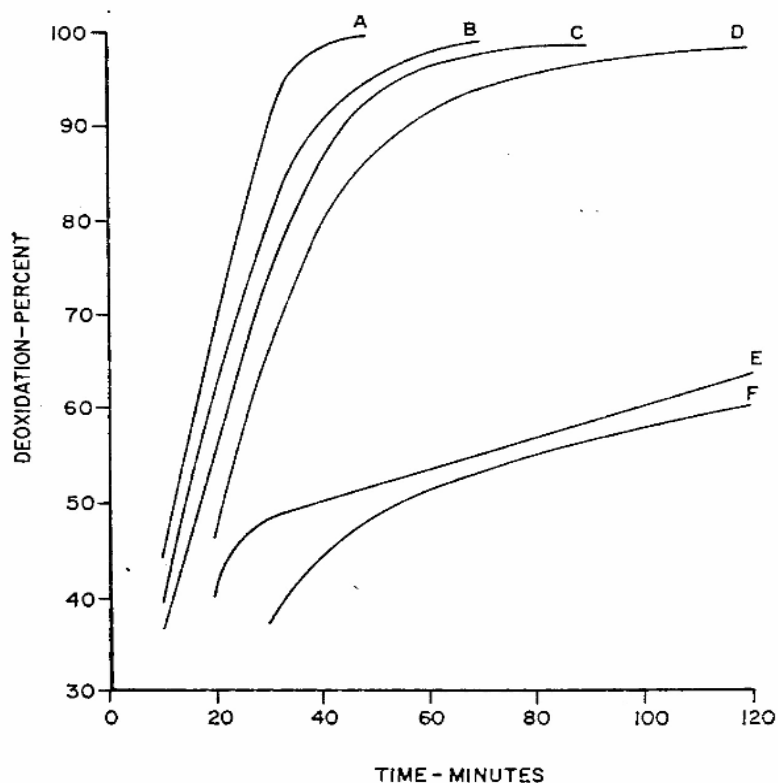


Figure 2.1 Relative Reducibility of Blast Furnace Feeds

- A- Limonite Ore
- B- Hematite Ore
- C- Pellets
- D- Sinter
- E- Nodules
- F- Dense Magnetite Ore

### 2.4.3 Reduction Disintegration

It is extremely difficult to determine what happens to a pellet after it enters the blast furnace. Questions have arisen as to whether certain types of pellets might disintegrate in the furnace before they reached the smelting zone. Several tests have been advanced to measure this disintegration. One is the “Linder Test” developed by Rolf Linder of Sweden [5]. Linder attempts to simulate in a rotating drum the temperatures and type of atmosphere to which the pellet is exposed in

the blast furnace. The North American industry has, however, found little correlation of Linder test results with blast furnace performance.

The Gakushin test is widely used by the Japanese steel industry. Basically, this test differs from the Linder test in that it employs a single temperature, 1652 °F (900 °C) and a single atmosphere containing 30 % CO and 70 % N<sub>2</sub>. Results are determined by the weight of tested material remaining after screening at 3 and 28 meshes. Weight loss is used to calculate the degree of reduction. The extent of percent swelling is also measured.

Another test sometimes used to evaluate behavior of pellets is that devised by Holowaty and Squarcy [6]. Pellets are subjected to a compressive load while at high temperature and the amount of deformation is considered to be related to that which would be experienced in the blast furnace.

## **2.5 Sintering**

### **2.5.1 Process Description**

In sintering, a shallow bed of fine particles is agglomerated by heat exchange and partial fusion of the quiescent mass. Heat is generated by combustion of a solid fuel admixed with the bed of fines being agglomerated. The combustion is initiated by igniting the fuel exposed at the surface of the bed, after which a narrow, high temperature zone is caused to move through the bed by an induced draft applied at the bottom of the bed. Within this narrow zone, the surfaces of adjacent particles reach fusion temperature, and gangue constituents form a semi liquid slag. The bonding is affected by a combination of fusion, grain growth and slag liquidation. The generation of volatiles from the fuel and fluxstone creates a frothy condition and the incoming air quenches and solidifies the rear edge of the advancing fusion zone. The product consists of a cellular mass of ore bonded in a slag matrix.

## 2.5.2 Sinter Mineralogy

The nature of the bonding which affects agglomeration is of interest in that this bonding affects the economics of production, transportation, storage, handling and ultimately, the reduction in the blast furnace.

Sinter strength is strongly influenced by the textural relationship between slag glass, slag crystals and oxide phase. If the slag glass covers the oxide particle, the sinter is weakened, whereas, if the slag glass is confined to interstitial bridges to oxide particles, the texture is relatively stronger.

A sinter may be regarded as consisting of three types of materials: [7]

- a) Original, unaltered material (primary).
- b) Original mineral constituents which have altered their structure and shape through recrystallization in the solid state (secondary).
- c) Secondary constituents which result from material which has fused or dissolved during sintering. These constituents may either remain mutually dissolved or may precipitate from the solution.

Although the resultant mineralogy of a sinter is principally dependent upon the chemistry and the mineral character of the raw mix and the maximum process temperature to which the mix was exposed, such factors as time above the solidification temperature, cooling rate, and the sintering atmosphere affect the final mineralogy. Thus, it is necessary to possess a detailed process “history” of a sinter when attempting to relate resultant mineralogy to process evaluation.

Sinters of low basicity ( $<0.5$ ) are generally characterized by grains of primary and secondary hematite and of magnetite bonding by a slag phase. The slag phase is primarily a silicate glass (combinations of FeO, CaO,  $Al_2O_3$  and  $SiO_2$ ), but will contain fayalite ( $2FeO.SiO_2$ ), wollastonite ( $CaO.SiO_2$ ), iron monticellite ( $CaO.FeO.SiO_2$ ) and anorthite ( $CaO.Al_2O_3.2SiO_2$ ). The formation of fayalite is

promoted by high fuel contents [8]. This phase is considered objectionable, as it adversely affects the reducibility of a sinter. The proportion of the hematite is decreased and the phase rankinite ( $3\text{CaO}\cdot 2\text{SiO}_2$ ) is more likely to be encountered. Some monocalcium ferrite ( $\text{CaO}\cdot\text{Fe}_2\text{O}_3$ ) may be encountered, localized about the pores of the sinter [9] and scattered throughout, often growing as a fringe around magnetite.

As the sinter basicity is increased beyond 1.0, devitrification becomes an important attribute of the glass. Knepper [10] report a devitrification of the silicate glass bond at basicities between 1.0 and 1.2, with the separation of crystallites of dicalcium silicate ( $2\text{CaO}\cdot\text{SiO}_2$ ) and the appearance of a calcium ferrite constituent. As the basicity is further raised to 1.8, the amount of silicate glass decreases, with increasing amounts of dicalcium silicate and calcium ferrites appearing. Above 1.8 basicity, the amount of calcium ferrites in the bond is increased, and the proportion of dicalcium silicates decreased to dilution. Kissin and Litvinova [11] report that the main minerals in the sinters of different basicity are hematite, magnetite, monocalcium ferrite, and iron-calcium olivine of composition  $\text{Ca}_x\text{Fe}_{2-x}\text{SiO}_4$  with the value of  $x$  increasing from 0.25 to 1.75 as the basicity is increased.

In a final analysis, the dependence of sinter strength and reducibility on the sinter mineralogy and mineralogical bonding which is achieved is reflected in sinter plant and blast furnace economics. It is the proper mineralogical assemblage that enables a sinter to withstand degradation during transit, storage, and descent within the blast furnace, yet gives the reduction and structural properties necessary for rapid reduction by the blast furnace process. Within the sinter plant, proper mineralogy can influence such processing and economic factors as fuel requirement and amount of returns to be reprocessed.

### **2.5.3 Sinter Quality**

#### **2.5.3.1 Sinter Size Consist**

The size consist of sinter has a significant effect on blast furnace performance. There is no universally recognized optimum sinter size, but it is certainly accepted that fines are detrimental to furnace operation. Fine material lowers blast furnace stack permeability, increases dust losses, and may lower the maximum permissible blast temperature for smooth furnace operation. Sinter that is too coarse is also undesirable, particularly if its reducibility is low and it is poor in strength, thus undergoing physical degradation during furnace processing.

#### **2.5.3.2 Sinter Strength**

Strength is a prime factor in assessing overall sinter quality, and is often the single index for such an assessment. Because there is no standard test in the United States for the determination of sinter strength, several tests have been developed for determining the strength and the significance of a given testing technique. Virtually all testing techniques have been limited to the measurement of the strength of cold sinter. The importance of the “hot strength” of sinter is realized, but little success has been achieved in developing techniques for its determination.

The most common techniques for assessing the strength of cold sinter may be grouped into three categories. These are drop tests, impact tests, and tumble tests. Each is briefly described as follows;

- a) Drop of Shatter Test – A specified weight of sinter dropped a predetermined number of times from a fixed height. Generally, the amount of sinter tested is less than 100 pounds, but may be the entire cake produced from a laboratory batch sintering facility. The height of drop

ranges 4 to 10 feet and the number of drops are from 1 to 4. Strength is normally defined as the percentage of resultant material larger than 3/8 or 1/4 inches, although, conversely, the fraction of sinter smaller than 20 or 28 mesh may be used, and defined as “dust index”. This test is an adaptation of the coke drop shatter test [12] and was used as early as 1933 by Joseph, Barrett, and Wood [13].

- b) Impact Test – A specific object of specified weight and dimension is dropped a fixed distance onto a specified weight and size of sinter. The most common quantities employed are a 150 pound steel bar weight, a height of 53-1/2 inches, and a 1 pound sample of minus 1.050 plus 0.263 inch sinter. Complete descriptions and evolutions of this technique have been presented by Hamilton and Ameen [14] and Morissey [15]. Results are interpreted by the fraction of resultant material larger than 0.132 inches (6 mesh) or the mean particle size. A variation in the test has been employed by Holowaty, Goldfein and Sheets [16].
- c) Tumble or Abrasion Test – A specified weight and size of material is revolved in a drum for a fixed number of revolutions. Invariably, an A.S.T.M. coke tumbling drum is employed, which revolves at  $24 \pm 1$  revolution per minute. The tumble test has been specifically evaluated by Powers [17].

### **2.5.3.3 Reducibility**

The reducibility of sinter is governed largely by its porosity and mineralogical composition. Nonoccluded porosity is a measure of the surface available for gas-solid contact.

Sinter mineralogy has dominant effect on reducibility. Low FeO content has long been used as an “index” of good reducibility, since FeO reacts with silica to form the difficult to reduce phase fayalite. Fayalite formation can be reduced by the

addition of lime, which combines the silica as crystalline of lime and lime-iron, and as noncrystalline silicate glasses. Highly oxidized sinters are generally easier to reduce, especially if a large portion of the hematite has been formed by reoxidation of magnetite.

#### **2.5.3.4 Chemistry**

The best chemical criterion for sinter is a maximum iron content and minimum gangue content with suitable basicity, consistent with acceptable strength, reducibility, and blast furnace performance. The iron content is dependent almost entirely upon the ores which are available to the plant operator, and are usually selected for economic reasons other than those particularly associated with sintering. With the increased availability of high iron, low silica concentrates, sinters of 60 % iron and higher are not common.

### **2.6 Evaluation Properties of Burden Materials**

This part endeavors to review the present state of the test procedures developed to evaluate the properties of burden materials under the following main headings:

- physical properties of materials outside the blast furnace
- reducibility
- physical behavior during reduction

#### **2.6.1 Physical Properties of Burden Materials**

For burden materials outside the furnace, the most important factor is the physical or “cold strength”, that is, the resistance of a material to impact and abrasion.

The measurement of the strength of the burden materials is complex since strength can be measured as the resistance to shatter as the result of dropping, the resistance to abrasion, or compression strength; as a result following tests have been developed.

### 1. Shatter Test

The shatter test, which was developed for coke, is employed to determine the strength of sinters and ores. A typical shatter test is one in which 50 kg of an ore or sinter greater than 10 mm in size is dropped four times from a height of 2 m. The material is then screened and the shatter index expressed as the percentage of the material greater than 10 mm surviving. Shatter indices in this test of 80-83 % are indicative of strong sinters.

The results of such a shatter test can be readily correlated to tumbling and abrasion test results. The following correlation was obtained between the shatter test described above and the American Society of Testing Materials (A.S.T.M.) test procedures: [18]

+1/4 in. index on a United Kingdom sinter plant:

$$+10 \text{ mm shatter index} = 39.082 + 0.570 (\text{A.S.T.M. } +1/4 \text{ in. index}) \quad \text{Eq.2.1}$$

### 2. Tumbling and Abrasion Tests

The shatter test is being superseded by the A.S.T.M. test procedure in America and the United Kingdom, whilst analogous Micum tests are employed in Europe. The A.S.T.M tumbling and abrasion procedure consists of subjecting 11.3 kg of - 2 in. +3/8 in. (- 51 + 9.5 mm) sinter or ore, or -3/2 in. +1/4 in. (- 38 + 6.3 mm) pellets to 200 revolutions at 25 revolutions per minute in a drum 36 in. (915 mm) in diameter and 18 in. (458 mm) in length. The drum is fitted with two equally spaced lifters 2 in. (51 mm) in height. The abrasion or strength index is



given by the percentage weight of +1/4 in. (6.3 mm) material surviving the test , and the dust index by the percentage of - 30 mesh (595 μm) material produced.

The basic features of the A.S.T.M., the Micum and the Half-Micum, and the proposed International Standards Organization (I.S.O.) test procedures are given in Table 22. The size range of the samples used in the Micum and the Half-Micum tests, and the test indices, vary considerably, and the data given are typical examples. It will be noted that the A.S.T.M. test is carried on – 2 in.+3/8 in.(- 51 + 9.5 mm) sinter (or ore), whilst the proposed I.S.O. test treats the – 1.57 in.+ 0.39 in. (- 40 mm + 10 mm) fraction and this can preclude a considerable quantity of a given material. As, however, the top size of burden material is being reduced in modern practice, the amount of material excluded from the test will be reduced.

The various tumbling and abrasion test results can also be correlated. An investigation in the United Kingdom by BISRA [1] showed that a range of sinters, sampled and prepared as for the A.S.T.M. test, gave identical + ¼ in. indices when tumble for 200 revolutions in the A.S.T.M. drum, or for 100 revolutions in the Half-Micum drum. The following correlations between the Micum and the Half-Micum + 10 mm indices were also obtained for materials – 40 + 10 mm in size:

Carol Lake pellets      Half –Micum(+ 10 mm index) = Micum (+10 mm index)

Eq.2.2

Sinter sample              Half-Micum index = 1.142 \* Micum index              Eq.2.3

Grangesberg ore            Half-Micum Index = 1.084 \* Micum index              Eq.2.4

Mano River ore              Half-Micum Index = 1.046 \* Micum index              Eq.2.5

When the I.S.O. test is developed, there is little doubt that this can be correlated to the tumble test previously employed.

In the series of A.S.T.M. tests, it was observed that the surviving + 3/8 in.(9.5 mm) material for most ores was at a higher level than sinter, even for ores which

gave the poorest + ¼ in.(6.3 mm) index. The – ¼ in. material produced from the sinters examined range from 20-40 per cent, whilst the majority of ores produced from 15-40 per cent of – ¼ in. material. A significant feature found in this work was that, whereas sinters produced from 5-10 per cent of - 595 µm material, many of the ores tested produced considerably more. Tumbling and abrasion tests have demonstrated that pellets are high quality products with regard to physical strength. Ores, though usually more resistance to degradation in size than sinter, can produce higher levels of - 595 µm fines than sinters or pellets in handling.

Some ores appear to be ideal of shipping as a closely sized product, whilst other ores, if carefully screened at the mine, may produce undesirable fines in transit. On arrival these fines have to be screened out and agglomerated, thus increasing ore treatment costs. It is considered that the shipment of such ores together with fines, which would act as a cushion, would reduce further breakdown. Tumbling and abrasion and shatter tests have demonstrated that, in transit from the ore preparation and the sinter plant to the blast furnace, sufficient degradation can occur to adversely affect furnace operation. This has led to the practice of screening burden materials prior to the blast furnace, in order to remove the – 0.2 in. (- 5 mm) fraction.

Table 2.2 Tumbling and Abrasion Tests

		A.S.T.M.	Micum	Half-Micum	Proposed I.S.O.
Sample Preparation		2 in.			40 mm
		1.5 in.			
Materials sieved on indicated screens		0.75 in.			25 mm
		0.5 in.			16 mm
		3/8 in.			10 mm
		0.25 in.			6.3 mm
	Sample Size Range employed as aliquots of above	Sinter	-2 + 3/8 in.	-40 + 10 mm or -25 + 10 mm	
	Pellets	-1.5 + 1/4 in.			
Weight sample		25 lb.	50 kg	25kg	15 kg
Drum diameter		36 in.	1000 mm	1000 mm	1000 mm
Drum length		18 in.	1000 mm	500 mm	500 mm
Number of lifters		2	4	4	2
Size of lifter (width)		2 in.	100 mm	100 mm	50 mm
Number of revolutions		200	100	100	200
Speed (rpm)		24±1	25	25	25±1
Screen analysis after test		3/8 in.	10 mm		6.3 mm
		0.25 in.	5 mm		
		30 mesh (595µm)	2.5 mm		28 mesh (500µm)
Indices					
<i>Abrasion</i>		+0.25 in.	+10 mm		+6.3 mm
<i>Dust</i>		-30 mesh (595µm)	-2.5 mm		-28 mesh (500µm)

### 3.Compression test

The compression strength is usually measured for pellets, but much less attention has been paid to ores and sinters. The work of Callender [19] demonstrated that the variability of pellets was such that a large number of pellets must be tested in order to get a mean value within  $\pm 30\text{lb}$  (13.5 kg) of the true mean compression strength with 95 per cent confidence limits.

It is desirable, to quote the mean, maximum and minimum values for compression strength, together with the standard deviation, after testing a number of pellets.

In order to overcome the problem of variability, a compression test has been developed at Sweden at the L.K.A.B. laboratories for determining the compression strength of burden materials. A sample of 10-15 mm material is dried at 105 °C and 2 kg of this material is placed in a steel cylinder with an inner diameter of 200 mm which is closed with a free running piston and equipped with a removable base. The cylinder is then placed in a press and a pressure of 100 tonnes is applied. The compressed sample is removed and the weight percentage of 5 mm material surviving is taken as an index of the compression strength. This index is claimed to be a very sensitive measurement of the ability of pellets and lump ore to withstand the handling in shipment. The value varies between 20 per cent for very friable pellets and about 75 per cent for very hard pellets. The method has good reproducibility and the standard deviation is about 1 per cent.

#### 4.Porosity

In pellets, the pores are aggregates of the voidage that exists between the large number of particles that constitute a pellet, and are therefore irregular in diameter. In ores, the porosity is largely dependent on the geological history of the ore, the chemical composition and crystal structure. Sinter porosity is in a different category in that sinter has macro-pores due to its physical condition, as well as micro-pores which are a function of chemical composition and the mode of production.

There are, by definition, two types of pores, open and closed, e.g., those which are open to the outer surface of the material and those that are entirely enclosed and can not be reached by fluids. The porosity of pellets or ores is normally expressed as the volume of pores as a percentage of the total volume of the material tested, and as yet there is no standard method for evaluating this property.

In the classical method, the property is determined by measuring first the true density (often called the powder density), using finely ground powder and a

pycnometer, and second, the apparent specific gravity or bulk density. In its simplest form the latter is determined by completely filling the open pores with a fluid then weighing it in air and immersed in the fluid.

Let  $W_a$  = weight of dry pellet,

$W_b$  = weight of pellet soaked with and suspended in the immersion fluid,

$W_c$  = weight of pellet soaked with immersion fluid and suspended in air,

$\rho$  = density of immersion fluid,

$\rho_t$  = true density or powder density

$\rho_t$  = mass/true volume Eq.2.6

The bulk volume is equal to the volume of solid material plus the volume of the open and closed pores,

$$\text{BulkVolume} = \frac{W_c - W_b}{\mathbf{r}} \quad \text{Eq.2.7}$$

Apparent volume = volume of solid material and closed pores Eq.2.8

$$= \frac{W_a - W_b}{\mathbf{r}}$$

Bulk density or apparent specific gravity,

$\rho_a$  = mass / bulk volume Eq.2.9

$$= \frac{W_a}{W_c - W_b} * \mathbf{r}$$

Apparent solid density = mass / apparent solid volume Eq.2.10

$$r_{as} = \frac{W_a}{W_a - W_b} * r$$

Apparent porosity = volume of open pores / bulk volume Eq.2.11

$$\begin{aligned} \epsilon_{ap} &= \frac{W_c - W_a}{W_c - W_b} * 100 \\ &= 100 * \left( 1 - \frac{\rho_a}{\rho_{as}} \right) \end{aligned}$$

True porosity,  $\epsilon_t$  = volume of open and closed pores / bulk volume Eq.2.12

$$= 100 * \left( 1 - \frac{r_a}{r_t} \right) \%$$

Sealed porosity = true porosity – apparent porosity Eq.2.13

There are several variations of the above method, using a liquid to effect complete penetration of the open pores, which are all slow and tedious to perform.

The Aminco–Winslow porosimeter can be used to measure the porosity of a pellet by forcing mercury under pressures ranging from 1.8 p.s.i.a to 15000 p.s.i.a (12 kN/m<sup>2</sup> to 103.5 MN/m<sup>2</sup>) into the open pores. The volume of mercury used is read directly from a calibrated capillary stem.

The size of the pore penetrated at a given pressure may be calculated by the Laplace equation:

$$pr = 2\alpha \cos i \quad \text{Eq.2.14}$$

where

$p$  = pressure,

$r$  = radius of opening,

$\alpha$  = surface tension of mercury,

$i$  = contact angle ( $140^\circ$ ) between the mercury and the pellet.

The total pore volume and the pore size distribution of a pellet in the range from  $97\ \mu\text{m}$  to  $0.01\ \mu\text{m}$  may be measured. Only one or two pellets can be tested at any one time and the operation takes about two hours to carry out, this method may be considered as an absolute or standard method.

The Allis Chalmers Mineralogy Laboratory has developed a technique using a Beckman air compression pycnometer, in which air at 2 atmospheres ( $203\ \text{kN/m}^2$ ) pressure is forced into the open pores of 20-25 pellets in a matter of seconds and the volume of the impenetrable portion of the pellets is determined. The apparent volume of the pellets is then determined using a liquid pycnometer, and the open-pore volume is ascertained by difference. The complete determination takes only about fifteen minutes to perform.

Typical porosity values for pellets range from 22-30 per cent, and such pellets have satisfactory reducibility.

Typical results for ores [20] are as follows:

Cassinga	16 %
Bellary	18 %
Itabira	4-7 %
Cerro Bolivar	13 %
Kiruna B	0 %
Tazadit	13 %

## 2.6.2 Reducibility Tests

The selection of a reducibility test depends on the use to be made of the results. For routine quality control the test should be as simple as possible, e.g., isothermal, with constant gas composition and flow rate in a static bed designed to ensure good gas-solid contact. Since the chemical analysis to determine the degree of reduction of materials is slow and requires considerable skill, determination of reducibility by loss in weight has much to recommend it. The modern trend is to use the above conditions, preheating the charge under nitrogen before reduction is commenced in order to minimize the breakdown of the charge. The reducibility data for a specific material thus obtained becomes as nearly as possible a function of the reducing gas composition, flow rate, temperature, and size of the charge.

The rate controlling step in the reduction of burden materials is generally considered to be the reduction of wustite in the 900–1000 °C range and this temperature range is widely employed at the present time.

The number of static bed reducibility tests is manifold but, before describing some of the most widely used modern tests, the Linder rotating furnace procedure, which may be regarded as one of the pioneer methods, will be discussed because of its impact on the development of more recent test procedures.



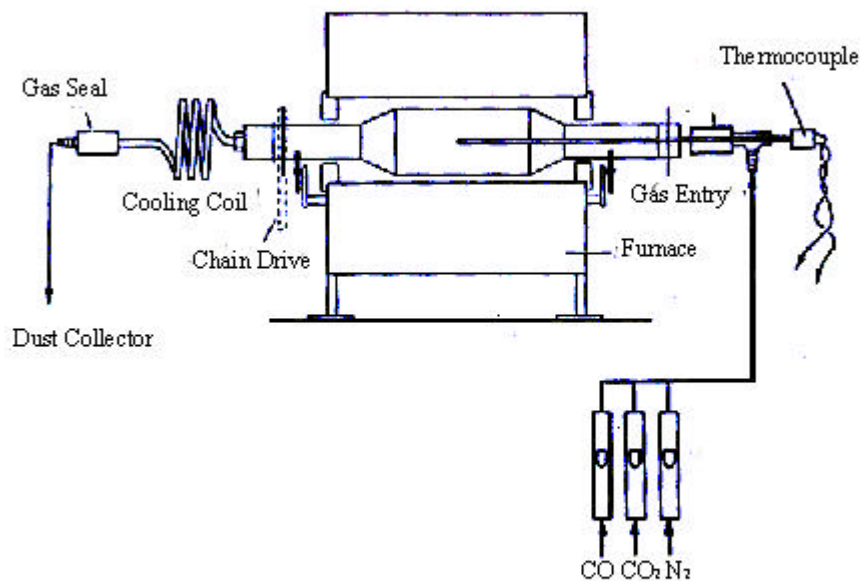


Figure 2.2 Linder Reduction Test Apparatus

The Linder test [5] was designed to determine the reducibility and break-down during reduction. The test consists of charging 500 g of carefully dried test sample together with 200 g of coke (30 – 40 mm in size) into a furnace (Figure 2.2), which is rotated at 30 revolutions per minute for 5 hours, and observing the following heating and gas composition cycles in an endeavor to simulate the descent of material in the blast furnace to the 1000 °C zone.

#### A) Temperature Cycle

0 – 2 hours temperature raised from room temperature to 700 °C

2 – 5 hours temperature raised from 700 to 1000 °C

## B) Gas Composition

	% CO	% CO <sub>2</sub>	CO / CO <sub>2</sub>
0 – 2 hours	30	10	3
2 - 4 hours	31.5	5	6.3
4 - 5 hours	32.5	2	16.25

The balance of the gas is nitrogen and the total gas flow rate is 15 liters / minute. After reduction, the tube is cooled under nitrogen and the sample is withdrawn. The coke is then separated by hand, and degradation of the reduced ore, determined by screen analysis, is usually recorded as the – 10 + 30 mesh (- 1676 + 500 μm) and - 30 mesh (- 500 μm) in the final product expressed as a percentage of the final product. The extent of reduction is determined by analyzing the reduced burden material for metallic, ferrous and ferric iron and using the following formula:

$$\text{Final Degree of Oxidation} = 100 * \left[ 1 - \left( \frac{\% \text{ ferrous iron}}{\% \text{ ferric iron}} - \frac{\% \text{ metallic iron}}{\% \text{ total iron}} \right) \right]$$

Linder claimed that the extent of reduction obtained in the test was the same as the extent of gaseous or indirect reduction obtained in the blast furnace, and cited tests and Swedish blast furnace data to show this.

The Linder test results, given in Table 2.3, show that magnetite ores are comparatively irreducible. On the other hand, hematite ores show a wide range of reducibility. Pellets are generally quite reducible. Sinters display a wide range of reducibility depending on the chemical composition (basicity) and the plant operating conditions.

Table 2.3 Typical Linder Test Results

		% Iron	Size Tested (mm)	Per cent Oxidation		Per cent Breakdown	
				Initial	Final	-1676µm	-500µm
1.	Hematite	52.9	12.5 - 25.0	99.8	39	2	4
2.	Hematite	65.0	12.5 - 25.0	99.7	67	6	12
3.	Hematite /Magnetite	58.5	12.5 - 25.0 12.5 - 25.0	94.5	71	10	5
4.	Magnetite	59.1	12.5 - 25.0	88.2	72	2	1
5.	Magnetite	58.8	12.5 - 25.0	89.8	75	20	28
6.	Hematite / Chamosite	55.7	12.5 - 25.0 12.5 - 25.0	93.8	58	14	19
<i>Pellets</i>							
A		67.4	15.0 - 25.0	99.6	49	6	2
B		66.3	8.0 - 10.0	99.7	54	1	1
C		63.0	6.0 - 12.0	99.8	52	3	2
<i>Sinters</i>							
United Kingdom		52.6	6.0 - 38.0	94.0	57	15	5
		59.1	6.0 - 38.0	96.7	42	26	14
		60.6	6.0 - 38.0	94.7	58	22	11

However, the test was not considered to be sensitive enough to discriminate adequately between the quality of the various grades of pellets on the market, nor was it suitable for use in test work where changes had been made to improve the pellet quality. The procedure also has three inherent features which are considered to lower the validity of the results:

1. The gas to solids contact does not simulate that in the blast furnace.
2. Breakdown occurs, and it is not possible to ascertain whether it occurs to the same extent as in the blast furnace or whether the reducibility affected in the test is correctly affected by the breakdown encountered.

3. Some materials in the partly reduced state can, on rolling, partly seal the surface or reseal cracks formed earlier in the test due to cracking, decrepitation or exfoliation.

As a result, the Linder test is being superseded as a reducibility test, but has been developed into a method of determining the low-temperature breakdown properties of burden materials.

### 2.6.2.1 Gakushin Test

This test was originally developed in Japan and there now exist several variations which have found extensive use (see Table 2.4) [21]. The apparatus is shown in Figure 2.3. Essentially, the dry sample is heated to constant weight in a vertical stainless steel cylinder, the base of which is packed with refractory beads which act as a gas preheater. The sample is heated to 900 °C under nitrogen, then the test gas is passed up through the sample at the required flow rate. In some cases the exit gas is analyzed continuously for carbon monoxide and carbon dioxide, though more recently reduction has been followed by a loss in weight technique.

Table 2.4 Various Versions of the Gakushin Method of Reducibility Testing

Version	Sample weight (g)	Test gas		Duration of test (hr)	Gas flow rate (l/min)	Test temp. (° C)	Test bed diameter (mm)
		CO %	N <sub>2</sub> %				
Official 1958	500	30	70	3	15	900*	60
Official 1960	600	30	70	3	16	900	75
Sumitomo	300	30	70	3	15	900	100
Yawata	300	30	H <sub>2</sub> , 2% max.	3	15	900	100
Nitrogen to balance							
Fuji	300	30		3	15	900	100
* 1650° F							

In addition to its use for measuring reducibility, the test has also been widely employed to measure (i) the break-down occurring during reduction, (ii) pellet swelling, and (iii) strength of materials after reduction. In this latter test the

reduced material is subjected to a small scale tumbling and abrasion test. One of the most recent variations in the Gakushin test is the Chiba reduction test [22] in which the following conditions are employed:

Sample weight	500 g
Sample size range	20-25 mm
Composition of reducing gas	33% CO, 67% N <sub>2</sub>
Reducing gas flow rate	20 l/min
Test temperature	900°C
Reduction time	100 min
Inner diameter of reaction vessel	68 mm

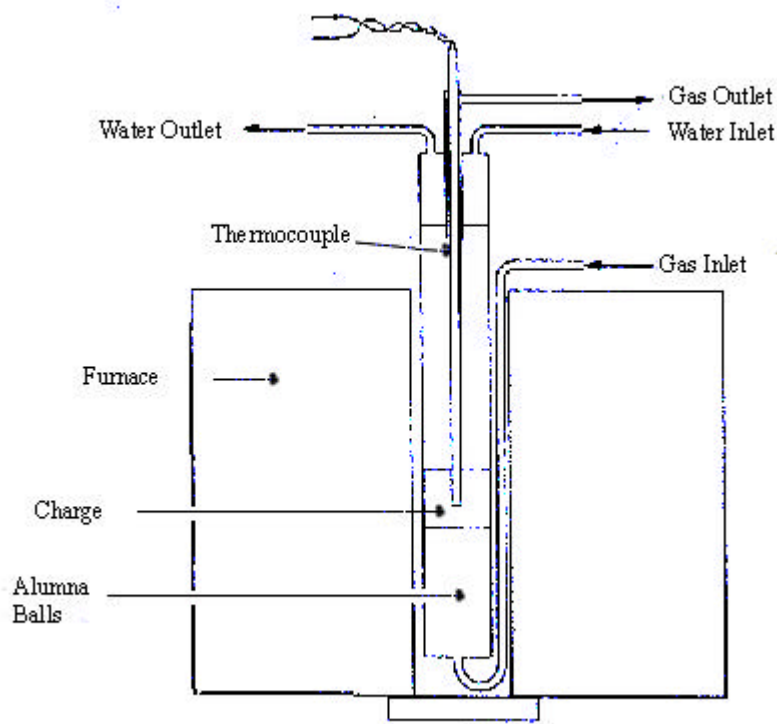


Figure 2.3 Gakushin Reduction Test Apparatus

The degree of reduction of the sample is calculated from the initial analysis of the sample and from the loss in weight, e.g., oxygen removed. The reducibility is expressed as an interface speed index  $k_i$  in mm/hour derived from the formula:

$$1 - (1 - F)^{1/3} = k_i * \frac{t}{d} \quad \text{Eq.2.15}$$

where;

F = degree of reduction effected expressed as a decimal fraction,

$k_i$  = interface speed (mm/hr),

$d$  = average particle diameter (mm),

$t$  = reduction time (hr).

Typical results are given in Table 2.5.

Table 2.5 Chiba Test - Reducibility Index Results

<i>(a) Reducibility of ores used in the U.K [18]</i>		<i>(b) Reducibility of ores used in the Japan [24]</i>	
<i>Ore Name</i>	<i>mm/hr</i>	<i>Ore Name</i>	<i>Mm/hr</i>
Svappavaara D	1.23	Jyoyo	1.42
Gellivare D	0.88	Bukkin	1.59
Tazadit	2.56	Dungun	1.88
F'Derik	2.04	Rompin	2.15
Cerro Bolivar	2.5	Temangan	3.44
Labrador'B'	2.98	Jorak	2.43
Hamersley	2.27	Goa	2.9
Kiruna B	1.08	Rhodesia	1.35
Mapava	2.26	Santa Fe	1.81
Itabira	1.72	Nevada	2.77
Grangesberg	1.01		
Wabana	1.29		
Djerissa	5.24		
Mount Newman	2.58		
Cassinga	1.77		

Kikuchi also derived a factor termed the “heat requirement for reduction per ton of iron” for a range of materials. This factor is derived from a heat and material balance and is based on the reducibility index, particle size and chemical composition of the material. It is employed to compare different burden materials and to obtain data on the optimum size range to be used.

### 2.6.2.2 Verein Deutscher Eisenhüttenleute (V.D.E.) Method

This is a static bed in which reduction is studied by a loss in weight technique [23]. A 1 kg sample, previously dried to constant weight at 105 °C, is placed in a stainless steel basket in a vertical cylinder, which is fitted with an external jacket, prior to passing up through the sample. The cylinder is suspended from a balance.

Reducing gas composition

CO 40 ± 0.5 %

N<sub>2</sub> 60 ± 0.5 %

CO<sub>2</sub> less than 0.2 %

O<sub>2</sub> not to exceed 0.1 %

Gas flow rate 5 normal m<sup>3</sup>/hr

Sample size 3-5 mm; 10-15 mm; 30-40 mm; 50-60 mm

The sample is preheated to 900 °C in an atmosphere of nitrogen then 60 per cent reduced, and readings of the loss in weight are taken at short time intervals.

Originally the reducibility index derived for this test was the rate of reduction (per cent/minute) after 40 per cent reduction had been effected, and was calculated using the following formula:

$$(dR/dt)_{40} = 33.6 / (t_{60} - t_{30}) \quad \text{Eq.2.16}$$

where;

$t_{60}$  = time (minutes) to attain 60% reduction,

$t_{30}$  = time (minutes) to attain 30% reduction.

With this procedure, however, materials were not being compared at the same state of oxidation, e.g., hematites were less reduced than magnetites. The

reducibility index is now measured or calculated as the rate of reduction (per cent/minute) when all materials are 60 per cent oxidized, e.g., when the atomic ratio O/Fe=0.9 and the results quoted as  $(dR/dt)_{60}$  (per cent reduction/minute).

Typical results obtained with this test are 0.5-1.0 per cent/minute for pellets. The reducibility of ores varies very much more widely.

### **2.6.2.3 Centre National de Recherches Metallurgiques (C.N.R.M.) Method**

This method is a static bed test in which the isothermal test temperature is 1000 °C [24,25]. The test conditions are as follows:

Bed diameter	58 mm
Sample weight	450 g
Sample size range	10-20 mm
Test gas composition	40% CO; 60% N <sub>2</sub>
Gas flow rate	1000 l/hr

This method differs from the V.D.E. method in that the rate of reduction is not followed during the test. After the test (duration one hour) the total amount of reduction is determined by chemical analysis of the reduced material or by weight loss.

### **2.6.2.4 Non-Isothermal Test: Aufheizverfahren Method**

The test apparatus (Figure 2.4) is similar to that for the C.N.R.M. test [26]. The only major difference is that the C.N.R.M. test gas is preheated electrically before it enters the reduction vessel. In the Aufheizverfahren test, the gas is preheated in the bottom part of the reduction vessel by passing through a layer of heated alumina pellets. The difference in the test procedures is that, unlike the C.N.R.M. test, the Aufheizverfahren test is not isothermal since the temperature is raised



linearly from 20 to 990 °C at 4 °C/minute. The test gas is made up of 35 per cent carbon monoxide and 65 per cent nitrogen. The course of the reduction is followed by equating the carbon dioxide evolved in the exit gas with oxygen loss from the sample. The vessel diameter is 50 mm, and sufficient dry sample, 10-15 mm in diameter to give a bed depth of 100 mm, is employed.

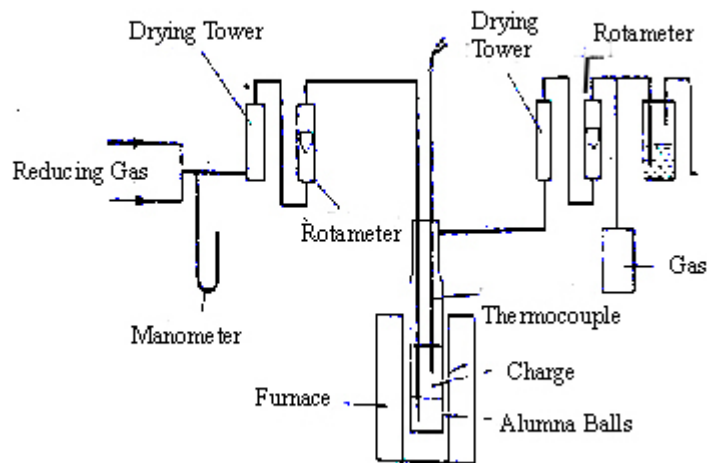


Figure 2.4 Aufheizverfahren Apparatus

#### 2.6.2.5 Determination of Reducibility by I.S.O. 4695

This standard is based on the following steps [27];

- a) Isothermal reduction of the test portion at a specified size range in a fixed bed, at a temperature of 950 °C using a reducing gas consisting of CO and N<sub>2</sub>.
- b) Weighing of the test portion at specified time intervals.
- c) Calculation of the degree of reduction relative to the iron (III) state and calculation of the rate of reduction at the oxygen /iron ratio of 0.9.

Composition of reducing gas shall consist of:

CO 40 % (V/V)  $\pm$  0.5 % (V/V)

N<sub>2</sub> 60 % (V/V)  $\pm$  0.5 % (V/V)

The reducing gas flow rate shall, during the test period, be maintained at 50 l/min  $\pm$  0.5 l/min

The test portion shall be reduced at a temperature of 950 °C.

The reducing gas should be preheated before entering the test portion at 950 °C  $\pm$  10 °C during the entire test period.

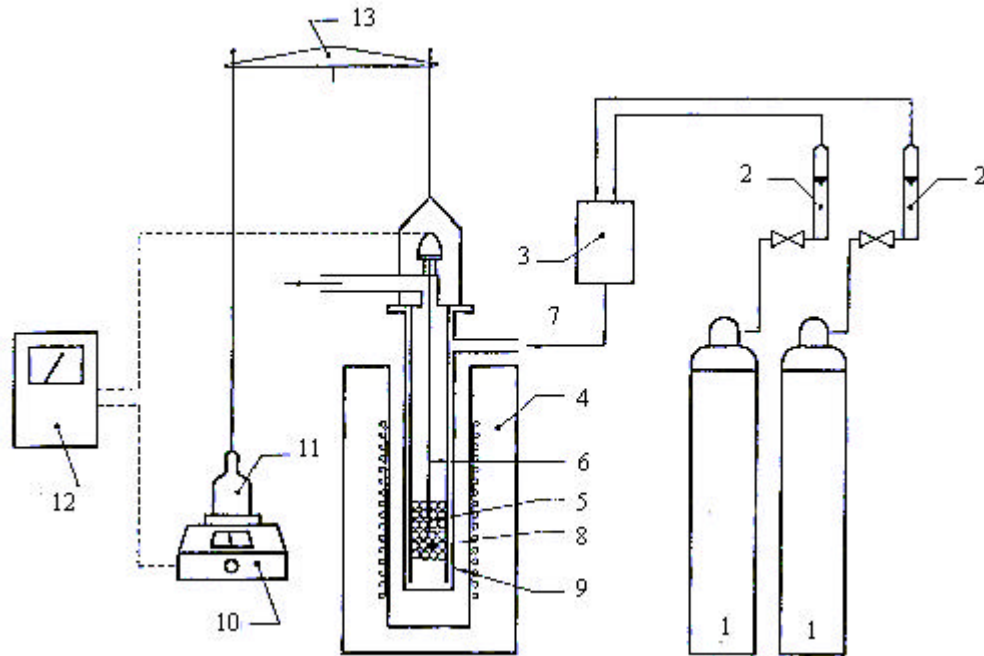
Weigh, to the nearest 1 g, approximately 500 g ( $\pm$  1 particle) of the test sample (mass  $m_o$ ).

Pellets should be sieved on 12.5 mm and 10 mm test sieves, discarding the + 12.5 mm – 10 mm fractions and retaining the – 12.5 mm + 10 mm.

Sinters and ores test samples should be in the size range – 12.5 mm + 10 mm.

Place the test portion, in the reduction tube, made of non-scaling, heat resistant metal to withstand temperatures of higher than 950 °C with a diameter of 75 mm  $\pm$  1 mm, so that the surface is even. In order to achieve a more uniform gas flow, a two-layer bed of porcelain pellets having a size range of 10 mm to 12.5 mm may be placed between the perforated plate and the test portion.

Close the top of the reduction tube. Insert the reduction tube into the furnace, having a heating capacity sufficient to maintain the entire test portion and the gas entering the bed 950 °C  $\pm$  10 °C, and suspend it centrally from the weighing device, ensuring that there is no contact with the furnace or heating elements.



Key

- 1) Gas cylinders with manometer and reduction valve
- 2) Gas flowmeters
- 3) Mixing vessels
- 4) Electrically heated furnace
- 5) Test portion
- 6) Thermocouple
- 7) Gas inlet
- 8) Layer of porcelain pellets
- 9) Double wall retort with perforated plate as sample holder
- 10) Digital balance
- 11) Load
- 12) Plotter for recording temperature and weight loss
- 13) Beam

Figure 2.5 Arrangement of a Test Unit for Determination of Reducibility According to I.S.O. 4695

Pass a flow of N<sub>2</sub> through the reduction tube at flow rate of approximately 25 l/min and commence the heating. When the temperature of the test portion approaches 950 °C increase the flow rate of the N<sub>2</sub> to 50 l/min. Continue the heating whilst maintaining the flow of the N<sub>2</sub> until the mass of the test portion is constant (mass  $m_1$ ) and the temperature is constant at 950 °C ± 10 °C.

Introduce the reducing gas to replace the N<sub>2</sub> at a flow rate of 50 l/min. Record the weight of the test portion at least every three minutes for the first 15 min and thereafter at 10 min intervals.

Terminate the reduction when the oxygen loss reaches 65 %. If, after 4 hours, this has not been achieved, the test may be stopped.

The degree of reduction after time  $t$ ,  $R_t$ , relative to the iron (III), as a percentage, can be calculated by the following equation:

$$R_t = \left[ \frac{0.111w_1}{0.430w_2} + \frac{m_1 - m_t}{m_0 * 0.430w_2} * 100 \right] * 100 \quad \text{Eq.2.17}$$

$m_0$  is the mass, in grams, of the test portion.

$m_1$  is the mass, in grams, of the test portion immediately before starting the reduction.

$m_t$  is the mass, in grams, of the test portion after reduction time  $t$ .

$w_1$  is the iron (III) oxide content, as a percentage by mass, of the test sample prior to the test and is calculated by multiplying it by a factor of 1.286.

$w_2$  is the total iron content, as a percentage by mass, of the test sample prior to the test.

Reduction curve can be prepared by plotting the degree of reduction  $R_t$  against time  $t$ .

Reducibility index can be read from the reduction curve the time in minutes to attain degrees of reduction of 30 % and 60 %.

The reducibility index, expressed as the rate of reduction at the atomic ratio of O/FeO of 0.9 (means a 40 % degree of reduction), in %/min, is calculated from the following formula:

$$\frac{dR}{dt}(O / Fe = 0.9) = \frac{33.6}{t_{60} - t_{30}} \quad \text{Eq.2.18}$$

where;

$t_{30}$  is the time to attain a degree of reduction of 30 % (min).

$t_{60}$  is the time to attain a degree of reduction of 60 % (min).

33.6 is a constant.

### **2.6.2.6 Iron Ores - Static Test for Low Temperature Reduction Disintegration**

#### **2.6.2.6.1 I.S.O. 4696-1: Reaction with CO, CO<sub>2</sub> and H<sub>2</sub>**

A test portion with a specified size range is subjected to static reduction at a temperature range of 500 °C using reducing gas consisting of CO, CO<sub>2</sub>, H<sub>2</sub> and N<sub>2</sub> [28].

After 1 hour reduction time, the test portion is cooled to a temperature below 100 °C and tumbled by using a small tumbler drum for 300 revolutions in total. It is then sieved with test sieves having square mesh apertures of 6.30 mm, 3.15 mm and 500 μm.

The reduction-disintegration index (RDI) is calculated as a quantitative measure of the degree of disintegration of an iron ore that has been reduced and tumbled: the percentage masses of material greater than 6.30 mm, less than 3.15 mm and

less than 500  $\mu\text{m}$ , respectively, are related to the total mass of the test portion after reduction and before tumbling.

The reducing gas shall consist of:

CO 20 % (V/V)  $\pm$  0.5 (V/V)

CO<sub>2</sub> 20 % (V/V)  $\pm$  0.5 (V/V)

H<sub>2</sub> 2.0 % (V/V)  $\pm$  0.5 (V/V)

N<sub>2</sub> 58 % (V/V)  $\pm$  0.5 (V/V)

The reducing-gas flow rate shall, during the test period, be maintained at 20 l/min  $\pm$  1 l/min.

The reducing gas shall be preheated before entering the test portion to maintain the test portion at 500 °C  $\pm$  5 °C during the entire test period.

Weigh, to the nearest 0.1 g, approximately 500 g ( $\pm$  1 particle) of the test sample.

The pellets in the size range of 10.0 mm to 12.5 mm shall be used for the test.

As same as pellets, sinters and ores in the size range of 10.0 mm to 12.5 mm shall be used for the test.

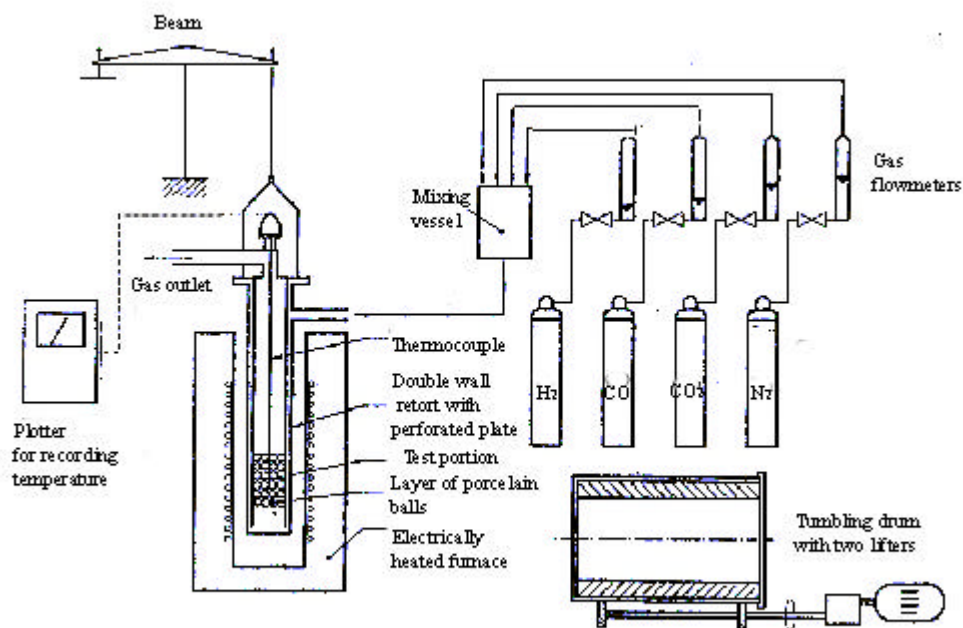


Figure 2.6 Arrangement of a Test Unit for I.S.O. 4696-1

Place a double-layer bed of porcelain pellets, having a size range of 10.0 mm to 12.5 mm, on the perforated plate.

Place the test portion on the porcelain pellets in the reduction tube, made of non-scarring, heat resistant metal to withstand temperatures of higher than 600 °C with a diameter of 75 mm ± 1 mm, and level the surface. Place the thermocouple in the centre of the test portion. Close the top of the reduction tube. Then insert the reduction tube into the furnace, having a heating capacity sufficient to maintain the entire test portion and the gas entering the bed 500 °C, and attach it to the weighing device of appropriate capacity and accuracy, to 0.1 g, ensuring that there is no contact with the furnace or heating elements.

Replace the air in the tube with inert gas. Heat the test portion and, while heating, pass a flow of inert gas through the test portion at a flow rate of approximately 20 l/min. Continue the heating, while passing inert gas, until the test portion reaches the test temperature of 500 °C ± 5 °C.

Introduce the reducing gas at a flow rate of 20 l/min  $\pm$  1 l/min to replace the inert gas and to reduce the test portion. Continue the reduction with the reducing gas for 1 h.

After 1 h reduction, stop the flow of the reducing gas and cool the test portion to a temperature below 100 °C in the reduction tube under a flow of inert gas.

Remove the test portion carefully from the reduction tube, determine the mass ( $m_0$ ) and place it in the tumbler drum. Fasten the lid tightly and rotate the drum for a total of 300 revolutions at a rate of 30 rev/min  $\pm$  1 rev/min.

Remove all material from the drum, determine the mass and hand sieve with care on 6.30 mm, 3.15 mm and 500  $\mu$ m sieves. Determine and record the mass of each fraction retained on the 6.30 mm ( $m_1$ ), 3.15 mm ( $m_2$ ) and 500  $\mu$ m ( $m_3$ ) sieve. Material lost during tumbling and sieving shall be considered to be less than 500  $\mu$ m.

The reduction-disintegration index RDI-1, expressed as a percentage by mass, is calculated from the following equations:

$$RDI - 1_{+6.3} = \frac{m_1}{m_0} * 100 \quad \text{Eq.2.19}$$

$$RDI - 1_{-3.15} = \frac{m_0 - (m_1 + m_2)}{m_0} * 100 \quad \text{Eq.2.20}$$

$$RDI - 1_{-0.5} = \frac{m_0 - (m_1 + m_2 + m_3)}{m_0} * 100 \quad \text{Eq.2.21}$$

where



$m_0$  is the mass, in grams, of the test portion after reduction and before tumbling.

$m_1$  is the mass, in grams, of the oversize fraction retained on the 6.30 mm sieve.

$m_2$  is the mass, in grams, of the oversize fraction retained on the 3.15 mm sieve.

$m_3$  is the mass, in grams, of the oversize fraction retained on the 500  $\mu\text{m}$  sieve.

#### **2.6.2.6.2 I.S.O. 4696-2: Reaction with CO**

A test portion with a specified size range is subjected to static reduction at a temperature of 550 °C using reducing gas consisting of carbon monoxide (CO) and nitrogen (N<sub>2</sub>) [29].

After 30 min reduction time, the test portion is cooled to a temperature below 100 °C and tumbled by using a small tumbler drum for 900 revolutions in total. It is then sieved with test sieves having square mesh apertures of 2.8 mm.

The reduction-disintegration index (RDI-2.2.8) is calculated as a quantitative measure of the degree of disintegration of an iron ore that has been reduced and tumbled: the percentage by mass of material less than 2.8 mm is related to the total mass of the test portion after reduction and before tumbling.

The reducing gas shall consist of:

CO 30 % (V/V)  $\pm$  0.5 % (V/V)

N<sub>2</sub> 70 % (V/V)  $\pm$  0.5 % (V/V)

The reducing-gas flow rate shall, during the test period, be maintained at 15 l/min  $\pm$  0.5 l/min.

The reducing gas shall be preheated before entering the test portion to maintain the test portion at  $500\text{ }^{\circ}\text{C} \pm 10\text{ }^{\circ}\text{C}$  during the entire test period.

Weigh, to the nearest 0.1 g, approximately 500 g ( $\pm 1$  particle) of the test sample.

The pellets in the size range of 10.0 mm to 12.5 mm shall be used for the test.

Sinters and ores in the size range of 16.0 mm to 20.0 mm shall be used for the test.

Place the test portion in the reduction tube, made of non-scaling, heat resistant metal to withstand temperatures of higher than  $600\text{ }^{\circ}\text{C}$  with a diameter of  $75\text{ mm} \pm 1\text{ mm}$ , so that the surface is even. Close the top of the reduction tube. Then insert the reduction tube into the furnace, having a heating capacity sufficient to maintain the entire test portion and the gas entering the bed  $550\text{ }^{\circ}\text{C}$ .

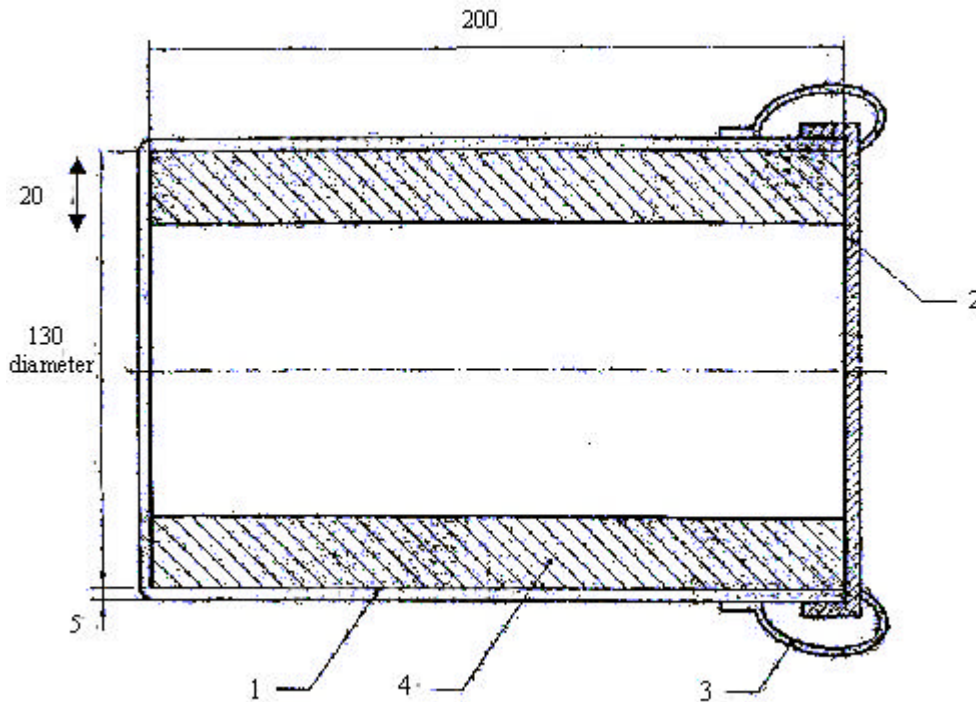
Replace the air in the tube with inert gas. Heat the test portion and, while heating, pass a flow of inert gas through the test portion at a flow rate of approximately 15 l/min. Continue the heating, while passing inert gas, until the test portion reaches the test temperature of  $550\text{ }^{\circ}\text{C}$ .

Introduce the reducing gas at a flow rate of 15 l/min to replace the inert gas and to reduce the test portion. Continue the reduction with the reducing gas for 30 min.

After 30 min reduction, stop the flow of the reducing gas and cool the test portion to a temperature below  $100\text{ }^{\circ}\text{C}$  in the reduction tube under a flow of inert gas.

Remove the test portion carefully from the reduction tube, determine the mass ( $m_0$ ) and place it in the tumbler drum. Fasten the lid tightly and rotate the drum for a total of 900 revolutions at a rate of  $30\text{ rev/min} \pm 1\text{ rev/min}$ .

Remove all material from the drum, determine the mass and hand sieve with care on a 2.8 mm sieve. Determine and record the mass of each fraction retained on the sieve ( $m_1$ ). Material lost during tumbling and sieving shall be considered to be  $-2.8$  mm.



#### Key

- 1) Vessel
- 2) Lid
- 3) Clamps
- 4) Frame with lifters
  - Lifters: 20 mm wide by 2 mm thick
  - Material: plain carbon steel

Figure 2.7 Example of Tumbler Drum for I.S.O. 4696-2. (Dimensions are in mm.)

The reduction-disintegration index  $RDI-2.2.8$ , expressed as a percentage by mass, is calculated from the following equations:

$$RDI - 2_{-2.8} = 100 - \frac{m_1}{m_0} * 100 \quad \text{Eq.2.22}$$

where

$m_0$  is the mass, in grams, of test portion after reduction and before tumbling.

$m_1$  is the mass, in grams, of oversize fraction retained on the 2.8 mm sieve.

### **2.6.2.7 I.S.O. 4697: Iron Ores – Test Method for Low Temperature Disintegration – Tumbling during Reduction**

This method is based on the following steps [30]:

a) Reduction of the test portion at a specified size range in a rotating tube at a temperature of 500 °C using a gas consisting of CO, CO<sub>2</sub>, H<sub>2</sub> and N<sub>2</sub>.

b) Cooling of the test portion, after 1 h reduction time, to temperature below 100 °C, and sieving with test sieves having square mesh apertures of 6.30 mm, 3.15 mm and 500 μm.

Calculation dynamic reduction-disintegration index (DRDI), as a quantitative measure of the degree of disintegration of iron ores that have been reduced during tumbling; the percentage mass of material greater than 6.30 mm, greater than 3.15 mm and less than 500 μm is related to the total mass of test portion after reduction.

The reducing gas shall consist of:

CO 20 % (V/V) ± 0.5 % (V/V)

CO<sub>2</sub> 20 % (V/V) ± 0.5 % (V/V)

H<sub>2</sub> 2.0 % (V/V) ± 0.5 % (V/V)

N<sub>2</sub> 58 % (V/V) ± 0.5 % (V/V)

The reducing gas flow rate shall, during the test period, be maintained at 20 l/min  $\pm$  0.5 l/min.

The pellets in the size range of 10 mm to 12.5 mm shall be used.

Sinters and ores in the size range of 10 mm to 12.5 mm shall be used.

Weigh, to the nearest 1 g, approximately 500 g ( $\pm$  1 particle) of the test sample.

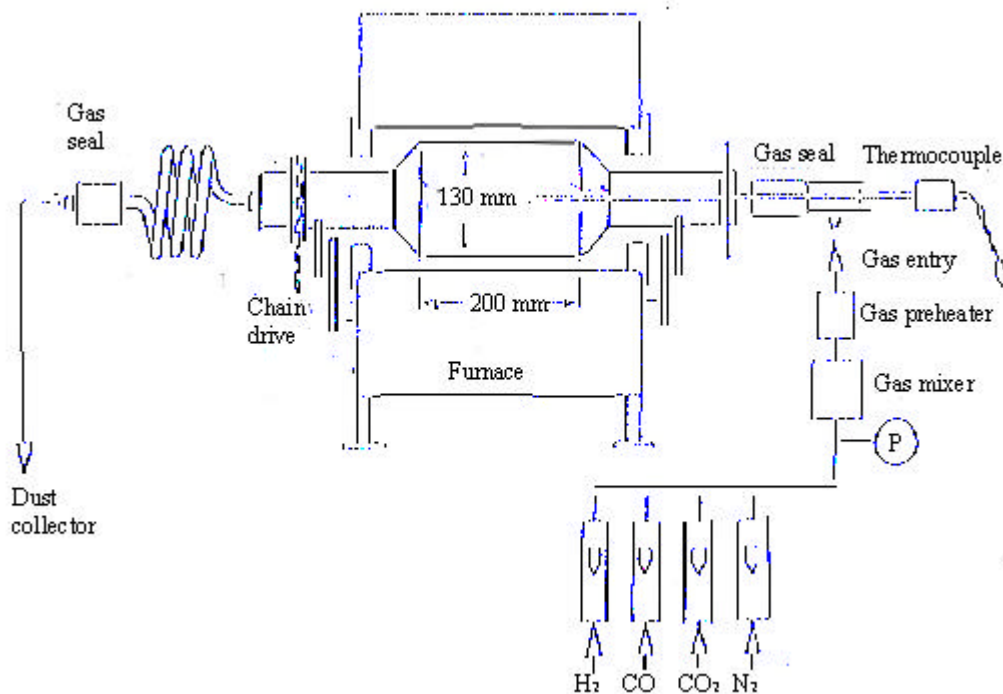


Figure 2 .8 Arrangement of Reduction Apparatus for I.S.O. 4697

Place the test portion in the reduction tube, made of non-scaling, heat resistant metal to withstand a temperature of 600 °C. Insert the reduction tube into the furnace and connect the gas flow system to the reduction tube. Commence rotation of the reduction tube at  $(10 \pm 1)$  rev/min.

Start a flow of nitrogen through the reduction tube at a rate of  $(20 \pm 1)$  l/min. Turn the power to the furnace on to heat the reduction tube and the test portion. The

heating rate shall be such that test portion reaches the test temperature of  $500 \pm 10$  °C in 45 min. Maintain the test temperature for 15 min to achieve temperature equilibrium.

Introduce the reducing gas at a flow rate of  $(20 \pm 1)$  l/min to replace the nitrogen and to reduce the test portion. Continue the reduction with the reducing gas for precisely 1 h.

After the 1 h reduction time, stop the tube rotation and the flow of the reducing gas and cool the test portion to a temperature below 100 °C in the reduction tube under a flow of nitrogen.

Remove the test portion from the reduction tube, determine the mass and hand sieve with care on 6.30 mm, 3.15 mm and 500 µm. Determine and record to the mass of each fraction retained. Material lost during sieving shall be considered to be minus 500µm. Determine the mass of the material collected in the dust collector.

The dynamic reduction-disintegration index, DRDI, expressed as a percentage by mass, is calculated from the following formula:

$$DRDI_{+6.3} = \frac{m_1}{m_0 + m_4} * 100 \quad \text{Eq.2.23}$$

$$DRDI_{+3.15} = \frac{m_1 + m_2}{m_0 + m_4} * 100 \quad \text{Eq.2.24}$$

$$DRDI_{-0.5} = \frac{(m_0 + m_4) - (m_1 + m_2 + m_3)}{m_0 + m_4} * 100 \quad \text{Eq.2.25}$$

where

$m_0$  is the mass, in grams, of test portion after reduction.

- $m_1$  is the mass, in grams, of oversize fraction retained on the 6.30 mm sieve.  
 $m_2$  is the mass, in grams, of oversize fraction retained on the 3.15 mm sieve.  
 $m_3$  is the mass, in grams, of oversize fraction retained on the 500  $\mu\text{m}$  sieve.  
 $m_4$  is the mass, in grams, of material collected in the dust collector.

#### **2.6.2.8 Determination of Relative Reducibility by I.S.O. 7215**

This method is based on the following steps [31]:

- a) Using carbon monoxide, isothermal reduction of the test portion placed on a balance in a fixed bed at 900 °C for 3 h.
- b) Heating and cooling in an inert atmosphere.

The reducing gas shall consist of:

- CO 30 % (V/V)  $\pm$  1.0 % (V/V)  
N<sub>2</sub> 70 % (V/V)  $\pm$  1.0 % (V/V)

The reducing gas flow rate shall, during the test period, be maintained at 15 l/min  $\pm$  0.5 l/min.

The reducing gas should be preheated before entering the test portion at 900 °C  $\pm$  10 °C during the entire test period.

Weigh, to the nearest 1 g, approximately 500 g ( $\pm$  1 particle) of the test sample (mass  $m_o$ ).

Pellets should be sieved on 12.5 mm and 10 mm test sieves, discarding the + 12.5 mm – 10 mm fractions and retaining the – 12.5 mm + 10 mm.

Sinters and ores should be in the size range – 12.5 mm + 10 mm.

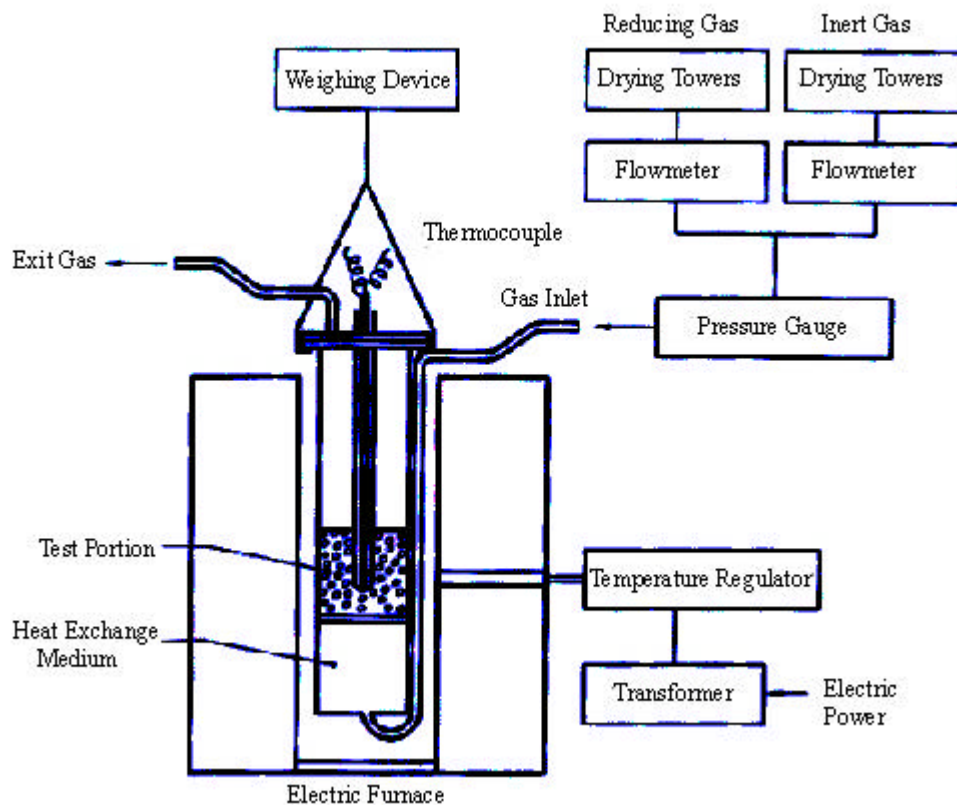


Figure 2.9 Schematic Diagram of Reduction Test Apparatus for I.S.O. 7215

Place the test portion in the reduction tube, made of non-scaling, heat resistant metal to withstand temperatures of higher than 910 °C with a diameter of 75 mm ± 1 mm, such that the surface is even.

Close the top of the reduction tube ensuring that the thermocouple is at the central position of the test portion. Insert the reduction tube into the furnace, having a heating capacity sufficient to maintain the entire test portion and the gas entering the bed 900 °C ± 10 °C, and suspend it centrally from the weighing device, capable of weighing the load to an accuracy of 0.5 g, ensuring that there is no contact with the furnace or heating elements. Connect the gas supply.

Pass a flow of N<sub>2</sub> through the reduction tube at a flow rate of approximately 5 l/min and start heating. When the temperature of the test portion approaches 900 °C increase the flow rate to 15 l/min and continue heating at 900 °C for 30 min.



Record the mass of the test portion ( $m_1$ ). Introduce the reducing gas to replace the  $N_2$  at a flow rate of 15 l/min.

At the end of 3 h reduction, determine the mass of the test portion ( $m_2$ ) and turn off the power.

The degree of reduction attained after 3 h (referred to as the final degree of reduction),  $R_f$ , expressed as a percentage, is given by the equation:

$$R_f = \left[ \frac{m_1 - m_2}{m_0(0.430w_2 - 0.111w_1)} \right] * 10^4 \quad \text{Eq.2.26}$$

where

$m_0$  is the initial mass, in grams, of the test portion.

$m_1$  is the mass, in grams, of the test portion immediately before starting the reduction.

$m_2$  is the mass, in grams, of the test portion after 3 h of reduction.

$w_1$  is the iron (II) oxide content, as a percentage by mass, of the test sample prior to the test and is calculated from the iron (II) content by multiplying by a factor of 1.286, determine in accordance with ISO 9035.

$w_2$  is the total iron content, as a percentage by mass, of the test sample.

The final degree of reduction,  $R_f$ , expressed as a percentage, shall be reported as the arithmetic mean of all test results, rounded to the nearest whole number.

### 2.6.2.9 I.S.O. 7992: Determination of Reduction Properties under Load

This method is based on the following steps [32]:

- a) Reduction of a bed of the test portion (test bed) with specified size by a carbon/hydrogen gas mixture at a temperature of 1050 °C, whilst applying a static load.
- b) Monitoring, at regular intervals, the loss in mass of test portion, and the differential gas pressure across the test bed and the height of the test bed.
- c) Determination of the differential pressure and the change in the height of the test bed at an 80 % degree of reduction.

The reducing gas shall consist of:

CO    40 % (V/V)  $\pm$  0.5 % (V/V)

H<sub>2</sub>    2.0 % (V/V)  $\pm$  0.5 % (V/V)

N<sub>2</sub>    58 % (V/V)  $\pm$  0.5 % (V/V)

The reducing gas flow rate shall, during the test period, be maintained at 83 l/min  $\pm$  1 l/min.

The reducing gas should be preheated before entering the test portion at 1050 °C  $\pm$  10 °C during the entire test period.

Weigh, to the nearest 1 g, approximately 1200 g of the test sample.

During the entire test period, the test portion shall be under a constant load of 50 kPa measured at the surface of the bed.

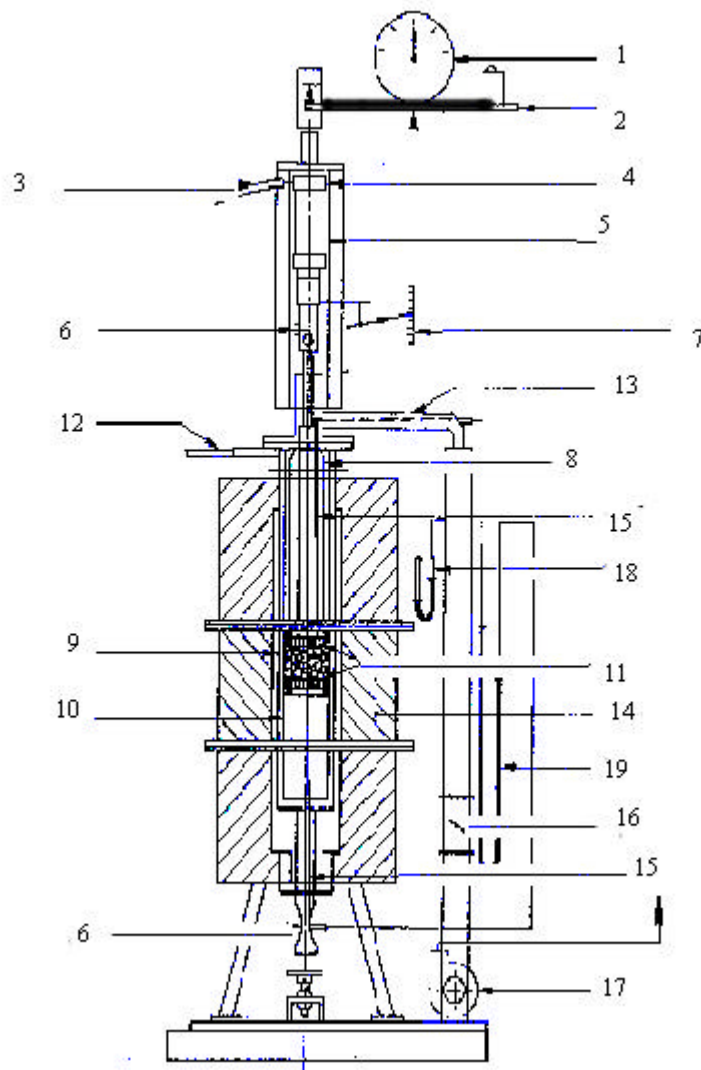
The pellets shall have the particle size between 10.0 mm and 12.5 mm.

The ores shall have the particle size between 10.0 mm and 12.5 mm.

Place a double layer bed of porcelain pellets with a size between 10.0mm and 12.5 mm on a perforated plate in the reduction tube, resistant to deformation, made of non-scaling, heat resistant metal to withstand temperatures of 1050 °C with a diameter of 125 mm  $\pm$  1 mm, in order to achieve uniform gas flow. After leveling, measure the height of the top surface of the porcelain layer. Place the test portion on the bed of porcelain pellets. After leveling, measure the height of the top surface of the bed of the test portion (test bed). Place a further double layer of porcelain pellets with a particle size between 10.0 mm and 12.5 mm on the test bed. After leveling, measure the height of the top of the surface of the porcelain layer again.

Close the top of the reduction tube by connecting the heat assembly containing the loading device to the reduction tube. Insert the reduction tube assembly into the furnace, having a heating capacity sufficient to maintain the entire test portion and the gas entering the bed 1050 °C  $\pm$  10 °C, and suspend it by the weighing device, capable of weighing the load to a sensitivity of 1g, centrally, ensuring that there is no contact with the furnace or heating elements.

Connect the thermocouple and the measurement devices for the differential pressure and for the change in the height of the test bed. Connect the gas supply system and the discharge line. Connect the loading device and apply a load of 50 kPa  $\pm$  2 kPa.



**Key**

- |                                |   |
|--------------------------------|---|
| 1) Scale                       | 11) Upper and lower perforated plates comprising the test portion |
| 2) Balance                     | 12) Reducing gas inlet  |
| 3) Compressed air inlet        | 13) Reducing gas outlet   |
| 4) Pressure cylinder           | 14) Main furnace body   |
| 5) Frame for pressure cylinder | 15) Differential gas pressure upper and lower probes              |
| 6) Thermocouple exit           | 16) Throttle valve  |
| 7) Linear scale                | 17) Waste gas fan   |
| 8) Loading ram                 | 18) Suction gauge   |
| 9) Outer reduction tube        | 19) Differential gas pressure manometer                           |
| 10) Inner reduction tube       |   |

Figure 2.10 Apparatus for Determining Reduction Properties under Load for I.S.O. 7992

Pass inert gas through the reduction tube at a flow rate of 50 l/min  $\pm$  1 l/min. When the temperature of the test portion approaches 1050 °C, increase the flow rate to 83 l/min. Continue heating until the mass of the test portion is constant and the temperature is constant at 1050 °C  $\pm$  10 °C.

Introduce the reducing gas to replace the inert gas at a flow rate of 83 l/min.

Measure and record the differential gas pressure across the test bed, the height of the test bed and the mass of the test portion at least every 5 min for the first 30 min and thereafter at 10 min intervals.

Terminate the reduction when the oxygen loss reaches 80 % of the value theoretically expected with an assumption that the entire test portion is pure iron (III) oxide.

Calculate the degree of reduction,  $R_t$ , relative to the iron (III) state after  $t$  min, expressed as a percentage, using the following equation:

$$R_t = \left[ \frac{0.111 * w(FeO)}{0.430 * w(Fe)} + \left[ \frac{m_1 - m_t}{m_0 * 0.430 * (Fe)} * 100 \right] \right] * 100 \quad \text{Eq.2.27}$$

where;

$m_0$  is the mass, in grams, of the test portion.

$m_1$  is the mass, in grams, of the test portion immediately before starting reduction.

$m_t$  is the mass, in grams, of the test portion after reduction time  $t$ .

$w(Fe)$  is the total iron content, expressed as a percentage by mass, of the test portion.

$w(FeO)$  is the iron (II) oxide content as a percentage by mass, of the test sample prior to the test and is calculated from the iron (II) content by multiplying by a factor of 1.286, determine in accordance with ISO 9035.

Using the reduction curve,  $R_t$  versus time, and the values of the differential gas pressure ( $p$ ), in kPa, obtained at different times ( $t$ ), plot the differential gas pressure against the degree of reduction. Read the differential pressure ( $p_{80}$ ) corresponding to an 80 % degree of reduction.

Using the height measurements taken during the test, calculate the percentage change in the height of the test bed ( $h$ ) obtained at different times. Plot the percentage change in the height of the test bed against the degree of reduction using the reduction curve. Read the percentage change in the height of the test bed ( $h_{80}$ ) corresponding to an 80 % degree of reduction.

#### **2.6.2.10 I.S.O. 13930; Dynamic Test for Low Temperature Reduction Disintegration**

A test portion with a specified size range is reduced in a rotating tube at a temperature of 500 °C using reducing gas consisting of carbon monoxide (CO), carbon dioxide (CO<sub>2</sub>), hydrogen (H<sub>2</sub>) and nitrogen (N<sub>2</sub>) [33].

The reducing gas shall consist of:

CO 20 % (V/V) ± 0.5 % (V/V)

CO<sub>2</sub> 20 % (V/V) ± 0.5 % (V/V)

H<sub>2</sub> 2 % (V/V) ± 0.2 % (V/V)

N<sub>2</sub> 58 % (V/V) ± 1 % (V/V)

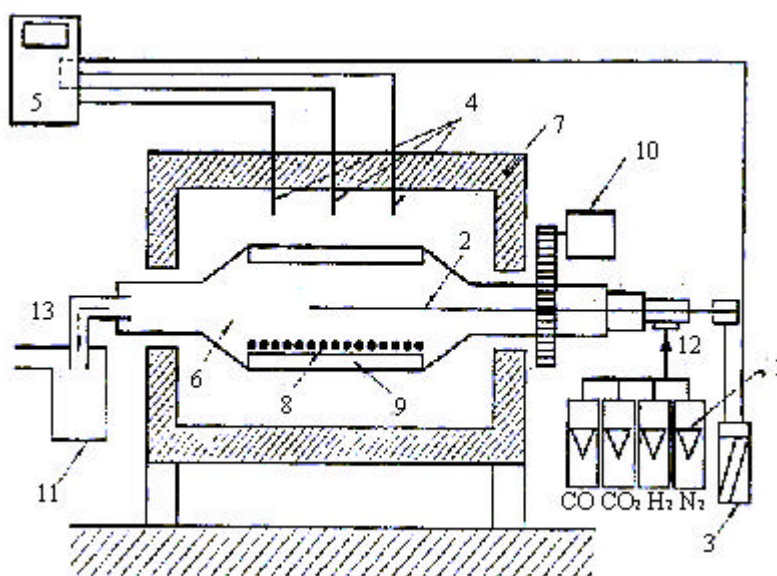
The reducing gas flow rate shall, during the test period, be maintained at 20 l/min ± 0.5 l/min.

The reducing gas should be preheated before entering the test portion at 500 °C ± 5 °C during the entire test period.

Weigh, to the nearest 1 g, approximately 500 g ( $\pm 1$  particle) of the test sample (mass  $m_o$ ).

Pellets in the size range of 10.0 mm to 12.5 mm and 12.5 mm to 16.0 mm shall be used.

Lump ores in the size range of 10.0 mm to 12.5 mm shall be used.



**Key**

- |   |                    |
|---|--------------------|
| 1) Gas flowmeters   | 7) Furnace         |
| 2) Thermocouple for measuring<br>reduction tube temperature | 8) Test portion    |
| 3) Temperature recorder                                     | 9) Lifter          |
| 4) Thermocouple for measuring<br>furnace temperature        | 10) Electric motor |
| 5) Temperature control unit                                 | 11) Dust collector |
| 6) Reduction tube, 540 mm * 150 mm,<br>four lifters         | 12) Gas in         |
|   | 13) Gas out        |

Figure 2.11 Low-Temperature Disintegration Test Apparatus for I.S.O. 13930

Place the test portion in the reduction tube, made of non-scaling, heat resistant metal to withstand temperatures of higher than 500 °C. Insert the reduction tube into the furnace and connect the thermocouple and the gas flow system to the reduction tube. Commence rotation of the reduction tube at 10 rpm  $\pm$  0.2 rpm.

Replace the air in the tube with inert gas. Heat the test portion and, while heating, pass a flow of inert gas through the reduction tube at a flow rate of approximately 20 l/min. Bring the temperature inside the reduction tube to 500 °C within 45 min and stabilize the temperature within the next 15 min. If this requirement is not met, discontinue the test and start a new one.

After a total time of 60 min, start the reduction. Introduce the reducing gas at a flow rate of 20 l/min  $\pm$  1 l/min to replace the inert gas and to reduce the test portion.

After 60 min reduction time, stop the flow of the reducing gas, stop the rotation of the reduction tube and cool the test portion to a temperature below 350 °C in the reduction tube under a flow (20 l/min) of inert gas. Then lift the reduction tube from the furnace and cool further, still under the flow of inert gas.

At a temperature below 100 °C, remove all the material from the reduction tube. Add the dust trapped in the dust collector to this material. Determine the mass ( $m_0$ ) to the nearest 1 g. Sieve mechanically on 6.3 mm, 3.15 mm and 0.5 mm sieves. Determine and record the mass of each fraction retained on the 6.3 mm ( $m_1$ ), 3.15 mm ( $m_2$ ) and 0.5 mm ( $m_3$ ) sieve. Material loss during sieving shall be considered to be -0.5 mm.

The low temperature disintegration indices  $LTD_{+6.3}$ ,  $LTD_{-3.15}$  and  $LTD_{-0.5}$ , expressed as a percentage by mass, shall be calculated to the first decimal place from the following equations:



$$LTD_{+6.3} = \frac{m_1}{m_0} * 100 \quad \text{Eq.2.28}$$

$$LTD_{-3.15} = \frac{m_0 - (m_1 + m_2)}{m_0} * 100 \quad \text{Eq.2.29}$$

$$LTD_{-0.5} = \frac{m_0 - (m_1 + m_2 + m_3)}{m_0} * 100 \quad \text{Eq.2.30}$$

where

$m_0$  is the mass, in grams, of the test portion after reduction including the dust trapped in the dust collector.

$m_1$  is the mass, in grams, of oversize fraction retained on the 6.30 mm sieve.

$m_2$  is the mass, in grams, of oversize fraction retained on the 3.15 mm sieve.

$m_3$  is the mass, in grams, of oversize fraction retained on the 0.5 mm sieve.

$LTD_{+6.3}$  the disintegration index expressed in terms of the mass % of the +6.3 mm sieve fraction (the so-called disintegration strength).

$LTD_{-3.15}$  the disintegration index expressed in terms of the mass % of the -3.15 mm sieve fraction (the so-called disintegration index).

$LTD_{-0.5}$  the disintegration index expressed in terms of the mass % of the -0.5 mm sieve fraction (the so-called disintegration abrasion).

### 2.6.3 Correlation of Reducibility Indices

In general the reducibility indices obtained by the various tests are comparable, and correlations have been derived between the Linder, C.N.R.M. and Aufheizverfahren indices. A broad correlation also exists between the Linder reducibility index and the V.D.E. index. There is no doubt, however, that the

adoption of a universally accepted international index of reducibility would greatly facilitate the comparison of data from all over the world.

## **2.7 The Effect of Agglomeration on Blast Furnace Operation**

In the last decade considerable effort has been devoted throughout the world to the measurement of reducibility, implying at that time reducibility was considered a major factor limiting blast furnace production.

For many years, the trend in sinter production had been to follow the example set in Scandinavia in striving for a high degree of oxidation in the sinter, which, as shown by laboratory work implied a high reducibility. Although little information exists relating the reducibility of burden materials with furnace coke rate, where such information does exist the effect is very small. Poos [34] claims that one degree of reducibility (C.N.R.M. test) is equivalent to 1.7 kg/tonnes of iron, whilst Linder [24] claims that one degree on the Linder scale is equivalent to 11 kg/tonnes.

Converting the C.N.R.M. results to the Linder scale by means of the formula, shows that the C.N.R.M. figures are equivalent to 2.3 kg/tonnes of iron:

$$R.Linder = 0.76 (C.N.R.M.) + 23.41 \quad \text{Eq.2.31}$$

In Japan, where the drive for high productivity has been as intense on the sintering plants as on the blast furnaces, high grade hematites have replaced magnetites in the sinter mix and, in order to maintain sinter strength, FeO contents of the sinter have been allowed to rise; a popular index of sinter quality for high blast furnace productivity is:

$$\text{Weight \% (FeO + SiO}_2\text{ + CaO)} = 27 \quad \text{Eq.2.32}$$

Yawata claims that an increase in the FeO content of sinter of 1 % is equivalent to an increase in coke rate of 0.032 cwt/ton (1.6 kg/tonnes) iron and that the FeO content of sinter should not exceed 8 %. Thus, in maintaining the above index of sinter quality and low FeO contents, additions of slag making materials to the sinter mix are deliberately made in the form of blast furnace slag.

Other factors apart from reducibility have an influence on the furnace coke rate. Improved gas/solid contact, brought about by changing the sequence of charging coke and sinter to the furnace, can have a greater influence than reducibility.

The present attitude towards sinter quality is to stress the importance of strength, narrow size range, and absence of – 0.2 in. (5 mm) fines rather than reducibility, particularly when fluxed sinter is being made from rich ores since such sinter is inherently of good reducibility. Yawata claims that a 1 % decrease in the – 0.2 in. (5 mm) fines content of the burden is equivalent to a decrease in coke rate of 0.118 cwt/ton (5.9 kg/tonnes), and it would thus appear that the benefits to be gained from uniform gas distribution in the stack through the absence of fines are far greater than those to be gained by improving the reducibility of individual lumps.

## CHAPTER 3

### EXPERIMENTAL

#### 3.1 Experimental Set Up for the Reducibility and Reduction Disintegration (RDI) Tests

Reducibility and reduction disintegration (RDI) tests of Erdemir samples were carried out by using the set up shown in Figures 3.1 and 3.2. The set up consisted of a tube furnace which was positioned vertically and heated by electricity, a stainless steel tube which was used as a test tube for this kind of furnace, a balance, gas flow meters and a container for the mixing of CO and N<sub>2</sub> gases [35]. The furnace, positioned vertically, consisted of three heating zones which could be controlled independently from each other and the furnace could be set at any desired temperature up to 1200 °C (±10 °C) by the help of these zones. As mentioned before, the test tube was made of stainless steel with an inside diameter of 65 mm and wall thickness of 2 mm. The length of the tube was 800 mm. The bottom of the test tube was welded with a stainless steel sheet of 2 mm wall thickness in order to close the end. A 10 mm outer diameter stainless steel pipe wound in spiral shape was used for heating of the inlet gases before entering the reduction tube and Al<sub>2</sub>O<sub>3</sub> balls contained in a 59 mm inner diameter and 63 mm outer diameter stainless steel tube closed at the bottom and at the top by perforated plates was placed at the bottom of reduction tube for uniform flow of gases through the system. The length of the Al<sub>2</sub>O<sub>3</sub> containing tube was 200 mm. The test sample was placed in the hot zone of the furnace on top of perforated plate for the determination of its reducibility. The stainless steel test tube was hung to a balance during the experiment. The balance had the capability of

measuring the weight change of test tube, generally 6 kg, and the specimen with the tolerances of  $\pm 500$  mg.

Key for the experimental set up given in Figure 3.1.

1	Gas tubes with manometers	5	Layer of alumina balls
2	Gas flow meters	6	Stainless steel tube
3	Mixing vessel	7	Mechanical balance
4	Electrically heated furnace	8	Test sample

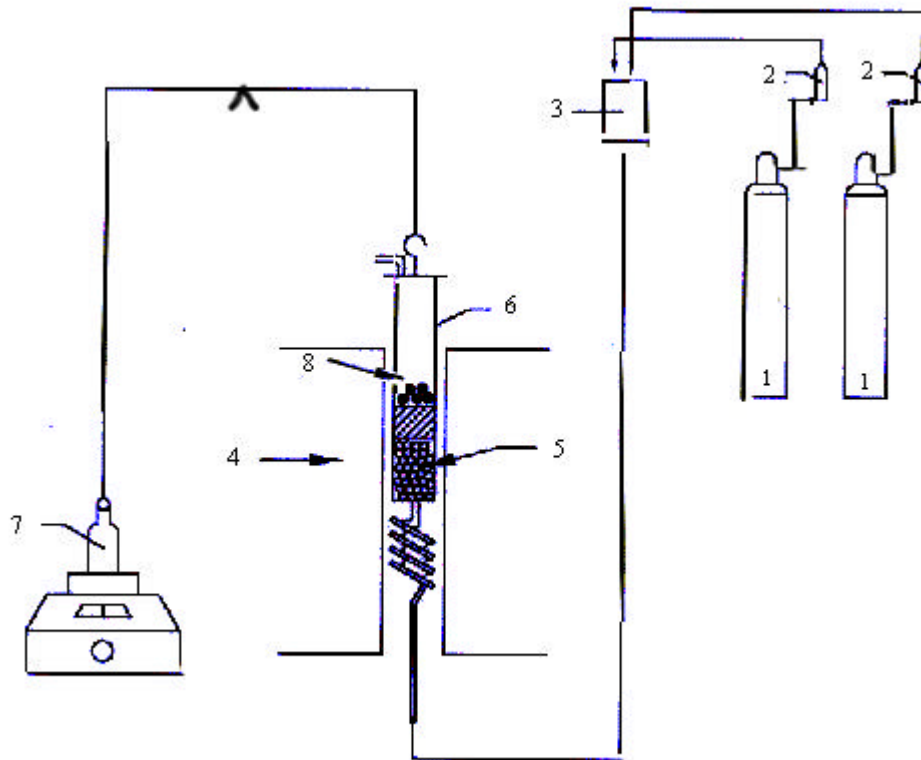


Figure 3.1 Set up for the Reduction and Reduction Disintegration Tests

Key for the stainless steel test tube and electrically heated furnace given in Figure 3.2.

1	Furnace	5	Test sample
2	Reduction tube	6	Gas inlet
3	Heating element	7	Gas outlet
4	Pipe filled with alumina balls		

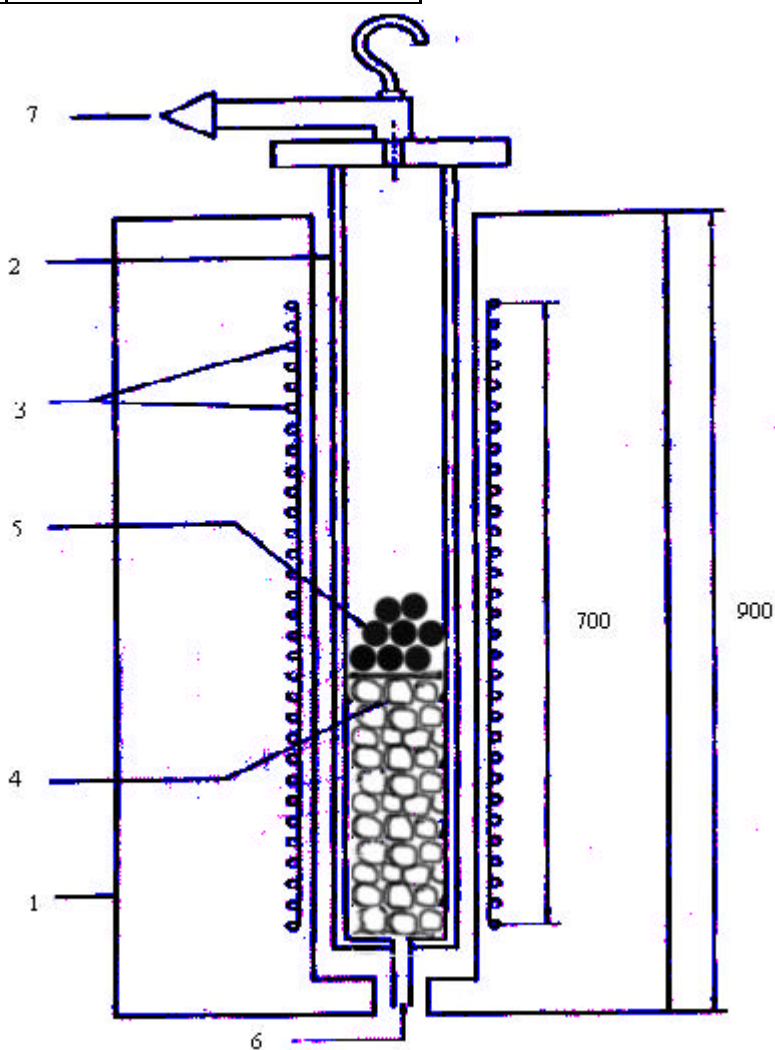


Figure 3.2 Experimental Set up Showing the Electrically Heated Furnace and the Test Tubes used in the Reduction and Reduction Disintegration Tests (Dimensions are in mm.)

### 3.2 Preparation of the Test Samples

Test samples used in the experiments were in the size range of 10-12.5 mm. Samples in amounts of 5 kg of each, were supplied by Erdemir Integrated Iron and Steel Works in this size range for the necessary experiments and measurements.

### 3.3 Measurement of True Density with Pycnometer

To determine the porosity of the specimens, their apparent and true densities were measured [36].

True density,  $\rho_t$ , is the proportion of the mass of the matter to its true volume. True volume is the volume of the solid part of a porous matter. To determine the true density of a crushed and ground sample, it is essential to know its true volume and mass.

For the determination of true density by using water pycnometer, some experimental tools were needed;

A) Pycnometer:

- Its capacity was 100 ml.
- Its stopper was shaved and had a capillary hole at the center.

B) Balance:

- It had the accuracy of  $\pm 0.0001$  g.

C) Drying Oven:

- Temperature of which could be set at  $110\text{ }^{\circ}\text{C} \pm 5\text{ }^{\circ}\text{C}$ .

D) Sieves:

- For screening the testing specimens from 2.8 mm and  $63\text{ }\mu\text{m}$ .

E) Liquid:

- Distilled water was used since;
- It would not react with the specimen.
- It had a known density.

For the determination of true density:

Initially, each sample was crushed to 2.8 mm size and then ground to a size so that all of the sample would pass through 63  $\mu\text{m}$  screen. During this sample preparation, it is important to prevent the specimen from moisture pickup and mixing of undesired substances during crushing and grinding.

For determining the mass of the specimen;

Firstly, the empty pycnometer was cleaned up and dried at 110  $^{\circ}\text{C}$ . Afterwards, it was essential to wait until the temperature of the pycnometer reached to room temperature. Then, the cleaned and emptied pycnometer was weighed within an accuracy of  $\pm 0.0001$  g including its stopper. After that, the dried specimen was placed up to one third of the pycnometer was filled.

Finally, the pycnometer, its stopper and specimen were weighed together with the accuracy of  $\pm 0.0001$  g. The difference between these weight measurements was the mass of the specimen ( $m_1$ ).

For determining the mass of pycnometer filled with liquid and specimen;

First of all, the pycnometer was filled with distilled water and glass stopper of the pycnometer was placed. Then, the overflowed liquid was cleaned carefully. Consequently, the pycnometer was weighed with the accuracy of  $\pm 0.0001$  g ( $m_2$ ).



For determining the mass of pycnometer filled with only distilled water;

After the determination of the mass of the pycnometer filled with liquid and specimen, the pycnometer was cleaned up and dried. Then, it was filled with distilled water and its weight was determined with the accuracy of  $\pm 0.0001$  g ( $m_3$ ). This procedure was repeated until the difference between the measurements was very small.

### **3.4 Measurement of Apparent Density with Mercury Pycnometer**

To determine the apparent density of sample, the procedure defined in TS 4379 was applied [37].

Apparent density is the proportion of the mass of the body to its apparent volume. Apparent volume is the sum of the volumes of the solid parts and porous parts of the body.

For the experiment, the following equipment was used;

A) Balance:

- It had a capacity of 5000 g with the accuracy of  $\pm 0.1$  g.

B) Drying Oven:

- It could be adjusted at temperature 105-110 °C.

C) Vacuum :

- Used to fill the pycnometer with mercury.

For the experiment, the specimens were used at their original size (between 10-12.5 mm), since, for the aspect of reducibility, the closed pores are important. Therefore, it is not wise to crush and grind these specimens. Otherwise, closed pores will vanish. The samples were dried at  $110 \text{ °C} \pm 5 \text{ °C}$  for 2 hours and approximately 20 g of sample was taken for each measurement. In order to avoid

the harmful effect of mercury vapor, the measurements were conducted in a ventilated area.

For the determination of apparent density;

Dry pycnometer, in Figure 3.3, was placed vertically so that its lower end was inserted into a bottle filled with mercury and the upper end was attached to the vacuum pump. First, the pycnometer was filled with only mercury and its weight was recorded ( $m_G$ ). It was emptied and nearly 20 g of 5-6 pieces of sample were placed inside the pycnometer. Afterwards, the pycnometer with the samples inside was filled with mercury again. During the filling operations, vibration was applied properly in order to force the mercury between the particles and open pores; also entrapped gas bubbles could go out of the chamber. The taps of the pycnometer were closed when mercury was on the reference level. The pycnometer with the sample inside filled with mercury was weighed and its weight was recorded ( $m_T$ ). The pycnometer was placed again for another measurement but first the mercury was emptied and another measurement was done without changing the sample. If the difference between the second and third measurements was negligible, the value could be recorded as the real value. Otherwise, the largest value was taken as the real value, since, the error would probably be the minimum in that measurement.

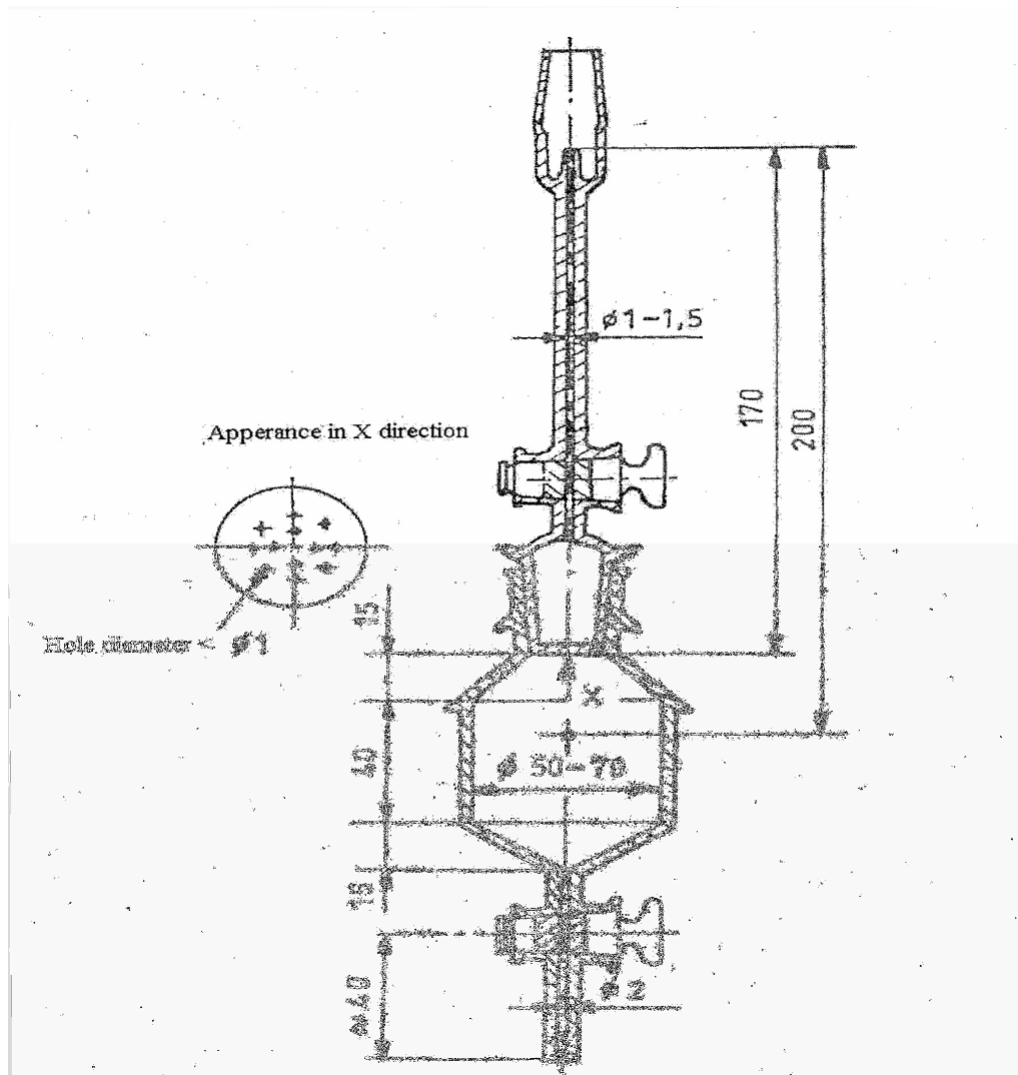


Figure 3.3 Drawing of the Mercury Pycnometer (Dimensions are in mm.)

### 3.5 Reducibility Test

For these tests, the Japanese standard JIS 8713 which is named as Gakushin test was carried out. A 500 gram sample of ore was, firstly, dried at 105 °C and then its weight was determined before it was placed into the test tube [35]. Top of the test tube was closed and hung to the balance. Afterwards, the connection of the tube and the gases, which would be passed through the system, was established. Then, N<sub>2</sub> gas was passed through the system at a flow rate of 5 l/min and the furnace was started to heat up. Under these circumstances, the temperature of the furnace was raised to 900 °C, the flow rate of N<sub>2</sub> gas was increased from 5 l/min

to 15 l/min. And, this amount of gas was passed through the system for at least ½ hour until no weight and temperature changes were observed. After stabilizing the weight of the sample at 900 °C, the flow of N<sub>2</sub> was stopped and the system was subjected to the reducing gas having 70% N<sub>2</sub> - 30% CO in composition. System was held at this temperature for 3 hours. It should be noted that, for the ores which have low reducibility, it would be better to hold the system at these circumstances for 4 hours. The weight loss of the specimen was measured with respect to certain time periods. After the reduction, the mixture of N<sub>2</sub> - CO gases passing through the system was cut off and instead of N<sub>2</sub> - CO mixture, N<sub>2</sub> gas was allowed to flow through the system with a flow rate of 5 l/min. System was cooled by the help of N<sub>2</sub> gas to below 100 °C. After finishing the reduction test, the reduced specimen was taken from the test tube and its weight was determined. For using the same specimen for another test, it should be mentioned that it must be preserved by preventing the air contact.

### **3.6 Reduction-Disintegration Test**

There are several reduction-disintegration tests being used by the iron and steel producers. Because of the availability of equipment in our Department, slightly modified ISO 4696-1 standard was chosen for determining the reduction-disintegration properties of the Erdemir samples in this study [28]. Test procedure was like the reducibility test. A 500 gram of sample was placed in the tube. N<sub>2</sub> gas was passed through the system at a flow rate of 5 l/min and furnace was started to heat up to 550 °C. Afterwards, the flow rate of N<sub>2</sub> gas was increased from 5 l/min to 15 l/min for 15 minutes. Then, 70% N<sub>2</sub> – 30% CO gas mixture was passed through the system for approximately 30 minutes. At the end of this period, the gas was cut off and a flow of 5 l / min of N<sub>2</sub> gas was allowed to pass through the system to cool the system to below 100 °C. Following the cooling step, the sample was removed from the system, it was weighed and put into a tumbler with the dimensions of 130 mm in inner diameter and 200 mm in length. Tumbler was rotated at a speed of 30 revolutions per minute for 30 minutes. Then, the sample was removed from the tumbler and screened. Finally, the weights of +6.7 mm,

-6.7 mm +3.35 mm and -3.35 mm +500  $\mu$ m fractions were determined. A drawing of the tumbler is given in Figure 3.4.

Key for the tumbler drum given in Figure 3.4.

1	Vessel
2	Lid
3	Clamps
4	Frame with lifters

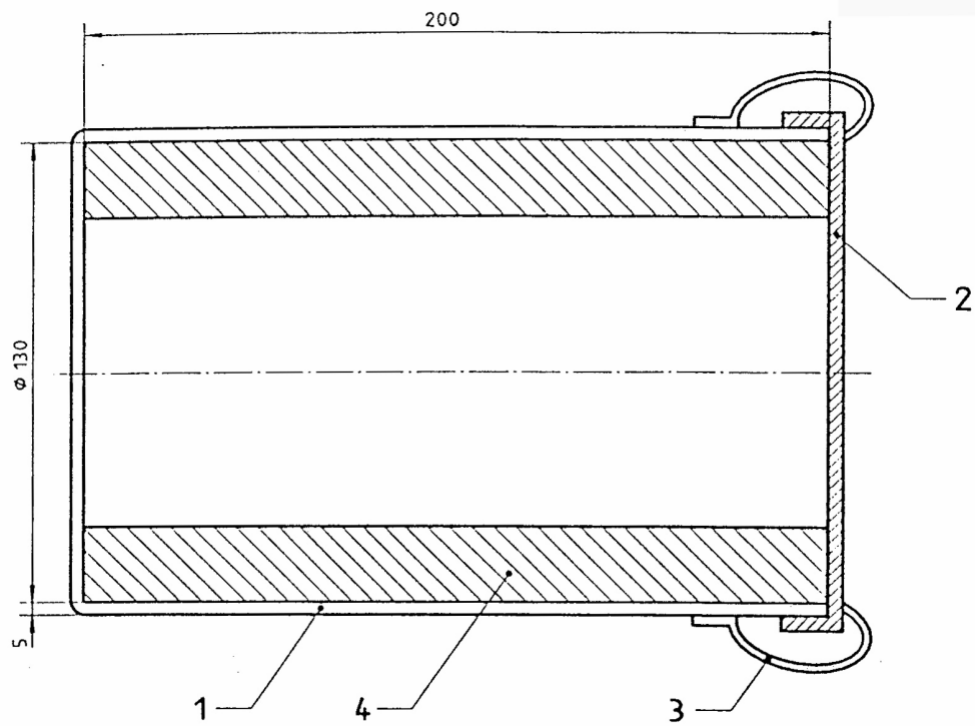


Figure 3.4 Drawing of the Tumbler Drum used in Reduction-Disintegration Test (Dimensions are in mm.)

## CHAPTER 4

### RESULTS AND DISCUSSIONS

#### 4.1 Mineralogical Structures and Chemical Compositions of Erdemir Samples

Mineralogical structures of Erdemir samples were determined by the help of X-ray diffraction (XRD) patterns. For comparison purposes, the mineralogical structure of some other local and imported iron ores, Divrigi pellet and Kardemir sinter studied in the past are also included in Table 4.1 together with those of Erdemir [39,41,42];.

Table 4.1 Mineralogical Structures of Erdemir Samples and the Others

Sample	Major Iron Minerals	Other Iron Minerals	Other Minerals
<i>Erdemir Lump Ore</i>	Hematite		
<i>Erdemir Pellet A</i>	Hematite		
<i>Erdemir Pellet B</i>	Hematite		
<i>Erdemir Sinter</i>	Wustite, Calcium Ferrite, Hematite&Magnetite		Dicalcium Silicate
<i>Kesikköprü</i>	Magnetite		Quartz
<i>Divrigi Concentrate</i>	Magnetite		Pyrite
<i>Divrigi (Dumluca)</i>	Hematite&Magnetite		Quartz
<i>DivrigiB-Kafa</i>	Hematite&Magnetite	Goethite	
<i>Divrigi Pellet</i>	Hematite		
<i>Akdag</i>	Hematite	Goethite	Calcite
<i>Attepe</i>	Hematite&Goethite	Limonite	
<i>Koruyeri</i>	Goethite&Hematite	Limonite	Calcite&Rhodochrosite
<i>Hekimhan</i>	Limonite	Goethite&Hematite	Quartz&Calcite
<i>Kardemir Sinter</i>	Wustite, Hematite &Magnetite		Dicalcium Silicate
<i>CVRD</i>	Hematite		
<i>ISCOR</i>	Hematite		

The chemical compositions of Erdemir samples provided by Erdemir Iron and Steel Works are given in Table 4.2.

Table 4.2 Chemical Compositions of Erdemir Samples

%	Lump Ore	Pellet A	Pellet B	Sinter
<i>Total Fe</i>	66.79	64.31	66.22	55.49
<i>FeO</i>	0.42	0.57	0.56	11.94
<i>SiO<sub>2</sub></i>	3.07	4.78	2.43	5.53
<i>Al<sub>2</sub>O<sub>3</sub></i>	0.50	0.34	0.40	2.18
<i>CaO</i>	0.07	2.18	1.91	10.30
<i>MgO</i>	0.02	0.28	0.21	1.52
<i>Na<sub>2</sub>O</i>	0.003	0.024	0.036	0.019
<i>K<sub>2</sub>O</i>	0.102	0.061	0.009	0.086
<i>TiO<sub>2</sub></i>	0.046	0.02	0.032	0.101
<i>Mn</i>	0.02	0.03	0.04	0.95
<i>P</i>	0.042	0.016	0.054	0.068
<i>S</i>	0.007	0.026	0.001	0.017
<i>As</i>	0.001	0.002	0.008	0.005
<i>Cr</i>	0.004	0.004	0.005	0.015
<i>Ni</i>	0.002	0.004	0.002	0.003
<i>Zn</i>	0.001	0.004	0.005	0.015
<i>Pb</i>	0.001	0.004	0.002	0.002
<i>Cu</i>	0.001	0.001	0.001	0.008
<i>Sn</i>	0	0	0.002	0
<i>V</i>	0	0.002	0	0

#### 4.2 Results of Apparent and True Density Measurements

For the reducibility and mechanical bond strength of iron ores, pellets and sinters, porosity is an important parameter. As mentioned, a porous iron oxide can be easily reduced rather than a compact one. Total porosity values of Erdemir samples were found by determining the true and the apparent density values.

True density was calculated by the given formula below;

$$r_t = \frac{m_1}{m_3 + m_1 - m_2} * r_1 \quad \text{Eq.4.1}$$

$\rho_t$  = true density of the specimen, g /cm<sup>3</sup>.

$\rho_1$  = density of the distilled water, g /cm<sup>3</sup>.

$m_1$  = mass of the specimen, g.

$m_2$  = mass of the pycnometer filled with liquid and specimen, g.

$m_3$  = mass of the pycnometer filled only with liquid, g.

The apparent density was calculated by a similar formula, given below;

$$B = \frac{m_p}{V_R} \quad \text{Eq.4.2}$$

where  $V_R$  ;

$$V_R = \frac{m_G + m_p - m_T}{r} \quad \text{Eq.4.3}$$

$V_R$  = apparent volume of the specimen, ml.

$m_G$  = mass of the pycnometer filled with only mercury, g.

$m_p$  = weight of the specimen, g.

$m_T$  = mass of the pycnometer filled with specimen and mercury, g.



$\rho$  = density of mercury, g/cm<sup>3</sup>.

By using the values found for true and apparent density, total porosity value, P, for each of the sample was calculated using the formula given below and porosity values that were obtained from the equation are reported in Table 4.3.

$$P = (1 - (d_A / d_T)) * 100 \quad \text{Eq.4.4}$$

$d_A$  : The apparent density of the sample, g /cm<sup>3</sup> .

$d_T$  : The true density of the sample, g /cm<sup>3</sup> .

Table 4.3 True Density, Apparent Density and Total Porosity Values of Erdemir Samples and the Other Samples

Sample	True Density (g/cm <sup>3</sup> )	Apparent Density (g/cm <sup>3</sup> )	Total Porosity (%)
<i>Erdemir Lump Ore</i>	4.46	4.10	8.1
<i>Erdemir Pellet A</i>	4.71	3.99	15.3
<i>Erdemir Pellet B</i>	5.14	3.42	33.5
<i>Erdemir Sinter</i>	5.02	3.84	23.5
<i>Kesikköprü</i>	4.43	4.18	5.6
<i>Divrigi Concentrate</i>	4.92	4.60	6.5
<i>Divrigi(Dumluca)</i>	4.93	4.50	8.7
<i>DivrigiB-Kafa</i>	4.65	4.27	8.2
<i>DivrigiPellet</i>	5.00	3.55	29.0
<i>Akdag</i>	4.43	3.84	13.3
<i>Attepe</i>	3.82	2.95	22.8
<i>Koruyeri</i>	3.65	2.72	25.5
<i>Hekimhan</i>	3.61	2.54	29.6
<i>Kardemir Sinter</i>	4.27	3.29	22.9
<i>CVRD</i>	4.90	4.20	14.3
<i>ISCOR</i>	4.95	4.78	3.4

### 4.3 The Results of Reduction-Disintegration Tests

In RDI tests, RDI  $_{-0.5}$  index is generally called the dusting index. RDI  $_{+6.7}$  and RDI  $_{+3.35}$  are the indices which show the strength of the samples. The calculations were made with the given formulas below;

$m_0$  = weight of sample before tumbling, g.

$m_1$  = weight of +6.7 mm sized particles, g.

$m_2$  = weight of -6.7 +3.35 mm sized particles, g.

$m_3$  = weight of -3.35 +500  $\mu$ m sized particles, g.

Reduction-disintegration indexes (RDI) of the samples are calculated by ;

$$RDI_{+6.7} = \frac{m_1}{m_0} * 100 \quad \text{Eq.4.5}$$

$$RDI_{+3.35} = \frac{m_1 + m_2}{m_0} * 100 \quad \text{Eq.4.6}$$

$$RDI_{-0.5} = \frac{m_0 - (m_1 + m_2 + m_3)}{m_0} * 100 \quad \text{Eq.4.7}$$

The RDI results of Erdemir samples together with those of others are given in Table 4.4 and Figure 4.1.

Table 4.4 RDI Values of Erdemir Samples and the Others

<b>Sample</b>	<b>RDI<sub>+6.7</sub></b>	<b>RDI<sub>+3.35</sub></b>	<b>RDI<sub>0.5</sub></b>
<i>Erdemir Lump Ore</i>	86.69	93.5	2.45
<i>Erdemir Pellet A</i>	96.18	97.81	1.92
<i>Erdemir Pellet B</i>	90.62	92.32	7.61
<i>Erdemir Sinter</i>	43.43	75.51	5.36
<i>Kesikköprü</i>	89.58	92.33	4.92
<i>Divrigi Concentrate</i>	95.37	96.35	1.7
<i>Divrigi(Dumluca)</i>	74.13	80.04	13.39
<i>DivrigiB-Kafa</i>	87.22	92.13	3.43
<i>Divrigi Pellet</i>	96.43	98.7	1.01
<i>Akdag</i>	82.12	89.56	5.19
<i>Attepe</i>	68.33	81.69	9.34
<i>Koruyeri</i>	72.92	83.52	8.36
<i>Hekimhan</i>	85.98	91.55	4.36
<i>Kardemir Sinter</i>	58.71	83.52	3.62
<i>CVRD</i>	71.82	83.55	7.71
<i>ISCOR</i>	96.86	98.7	0.4

High value of RDI<sub>0.5</sub> indicates a high amount of degradation at low temperatures during reduction. There are certain desirabilities which are the results of high value of RDI<sub>0.5</sub>;

- Gas permeability decreases in the furnace.
- Flow of gases becomes difficult.
- Dust amount increases at the stack gases.

RDI<sub>0.5</sub> values were given at Table 4.4. These values were not so high that these samples will not cause important problems during reduction at low temperatures. According to the results, Divrigi Dumluca had the highest RDI<sub>0.5</sub> which shows the highest amount of degradation during reduction at low temperature values.

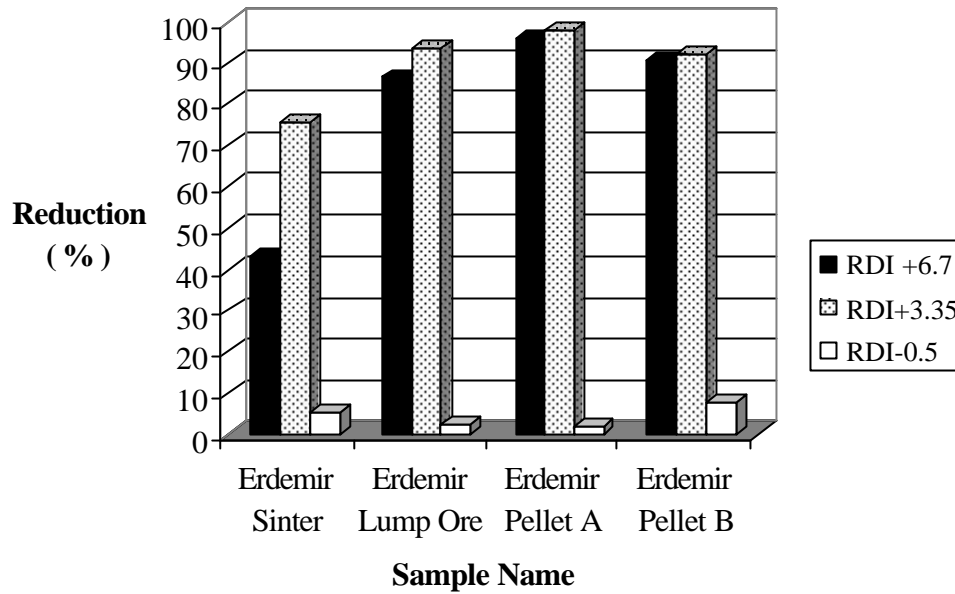
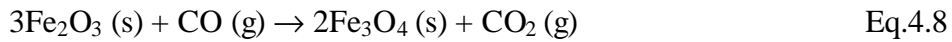


Figure 4.1 Results of the Reduction-Disintegration Tests of Erdemir Samples

#### 4.4 The Results of Reducibility Tests of Erdemir Samples

If CO - N<sub>2</sub> gas mixture is passed through an iron ore bed, iron oxides will be reduced according to reactions given below [38];



Due to these reactions, oxygen, combined with iron, will be removed from the sample. So that, there will be a reduction in the weight of the system which is exactly equal to the weight of oxygen removed from the system. During the experiment, one will measure the cumulative weight loss of the system with respect to time. Because of this, by measuring the cumulative weight loss of the system, the loss of oxygen with respect to time is observed from the experiment.

The percent reduction of iron ore;

$$\text{Reduction \%} = \frac{\text{Weight of oxygen removed from iron oxides by the reducing gas}}{\text{Total weight of oxygen bound to iron oxides before reduction}} * 100 \quad \text{Eq.4.11}$$

$m_k$  = weight of dried ore placed into the test tube, g

$m_o$  = weight of the ore in the test tube at 900 °C, just before the start of the reduction, g.

$m_t$  = weight of the ore in the test tube at any time t, g

Fe % = total weight percent of iron in the ore before the start of the experiment.

FeO % = weight percent of FeO in the ore before the start of the experiment.

$M_i$  = atomic or molecular weight of component 'i'.

Therefore, the denominator of Eq.4.11 will be equal to ;

$$m_o - m_t \quad \text{Eq.4.12}$$

Generally, iron ores (sinter and pellets) contain following iron oxides;

- FeO
- Fe<sub>3</sub>O<sub>4</sub> or (FeO. Fe<sub>2</sub>O<sub>3</sub>)
- Fe<sub>2</sub>O<sub>3</sub>

Therefore, the total oxygen content of an iron ore is the sum of the weight of the oxygen which is bound to FeO and the weight of oxygen which is bound to Fe<sub>2</sub>O<sub>3</sub>.

The weight of oxygen, found as FeO, is equal to ;

$$m_k * \frac{FeO \%}{100} * \frac{M_o (= 16)}{M_{FeO} (= 71.85)} \quad \text{Eq.4.13}$$

The weight percent of Fe as FeO can be expressed as;

$$FeO\% * \frac{M_{Fe} (= 55.85)}{M_{FeO} (= 71.85)} \quad \text{Eq.4.14}$$

So, the weight percent of Fe, bound to Fe<sub>2</sub>O<sub>3</sub>, will be equal to;

$$Fe\% - \left[ FeO\% * \frac{55.85}{71.85} \right] \quad \text{Eq.4.15}$$

Therefore, the weight of oxygen, found as Fe<sub>2</sub>O<sub>3</sub>, will be equal to;

$$m_k * \left[ Fe\% - \left( FeO\% * \frac{55.85}{71.85} \right) \right] * \frac{1}{100} * \frac{3 * M_o (= 3 * 16)}{2 * M_{Fe} (= 2 * 55.85)}$$

$$\text{Eq.4.16}$$

By the addition of equations 4.13 and 4.16, the total weight of oxygen, bound to iron, will be found as;

$$m_k * \left[ \left( Fe\% * \frac{48}{111.7} \right) - \left( FeO\% * \frac{8}{71.85} \right) \right] * \frac{1}{100} \quad \text{Eq.4.17}$$

If R % is defined as reduction percent for a certain time, t, by using equations 4.11, 4.12 and 4.17, it will be noticed that;

$$R\% = \frac{m_o - m_t}{m_k * \left[ \left( Fe\% * \frac{48}{111.7} \right) - \left( FeO\% * \frac{8}{71.85} \right) \right]} * 10^4 \quad \text{Eq.4.18}$$

By substituting in Fe % and FeO %, which are known from the chemical analysis of the ore;  $m_k$ ,  $m_o$  and  $m_t$  which are determined by the reduction test, with the use of Eq.4.18, it is possible to determine the percent reduction values with respect to time.

For expressing of the reducibility of iron ores, there exists a reducibility index. Both the rate of reduction of the iron ore and the rate of removal of oxygen, bound to Fe,  $dO/dt$ , are directly proportional to the amount of oxygen, bound to iron ore, therefore:

$$-\frac{dO}{dt} = k * O \quad \text{Eq.4.19}$$

Constant,  $k$ , in Eq.4.19 is defined as reducibility index.

$$R\% = \frac{O_o - O}{O_o} * 100 \quad \text{Eq.4.20}$$

$O_o$  = weight of oxygen, bound to iron ore, before the reduction, g.

$O$  = weight of oxygen at any time  $t$ , g.

By combining equations 4.19 and 4.20, it will be observed that;

$$\frac{dR\%}{dt} = k * \left[ 1 - \left( \frac{R\%}{100} \right) \right] * 100 \quad \text{Eq.4.21}$$

Then;

$$\frac{dR\%}{\left( 1 - \frac{R\%}{100} \right)} = 100 * k * dt \quad \text{Eq.4.22}$$

By integrating by parts;

$$\ln \left( 1 - \frac{R\%}{100} \right) = -k * t + const. \quad \text{Eq.4.23}$$

The slope of the graph,  $[-\ln(1 - (R\%/100))]$  versus  $t$  (time in minutes) will be the reducibility index,  $k$ .

From the above equations, percent reduction was calculated as a function of time.  $R\%$  obtained at the end of 3 hours, which is a measure of reducibility for different samples, are presented in Table 4.5. Percent reductions versus time data for the experimental Erdemir samples are presented graphically in Figures 4.2–4.6. For comparison purposes Erdemir samples are given all together in Figure 4.6.

Table 4.5 Reducibility Values of Erdemir Samples and the Others at the End of Three Hours

<b>Sample</b>	<b>Reduction % at the end of three hours</b>
<i>Erdemir Lump Ore</i>	43.4
<i>Erdemir Pellet A</i>	66.6
<i>Erdemir Pellet B</i>	78.7
<i>Erdemir Sinter</i>	77.6
<i>Kesikköprü</i>	40
<i>Divrigi Concentrate</i>	49
<i>Divrigi (Dumluca)</i>	56
<i>DivrigiB-Kafa</i>	63
<i>Divrigi Pellet</i>	72.5
<i>Akdag</i>	74
<i>Attepe</i>	92.2
<i>Koruyeri</i>	92.5
<i>Hekimhan</i>	91.5
<i>Kardemir Sinter</i>	69.6
<i>CVRD</i>	67.4
<i>ISCOR</i>	43.2



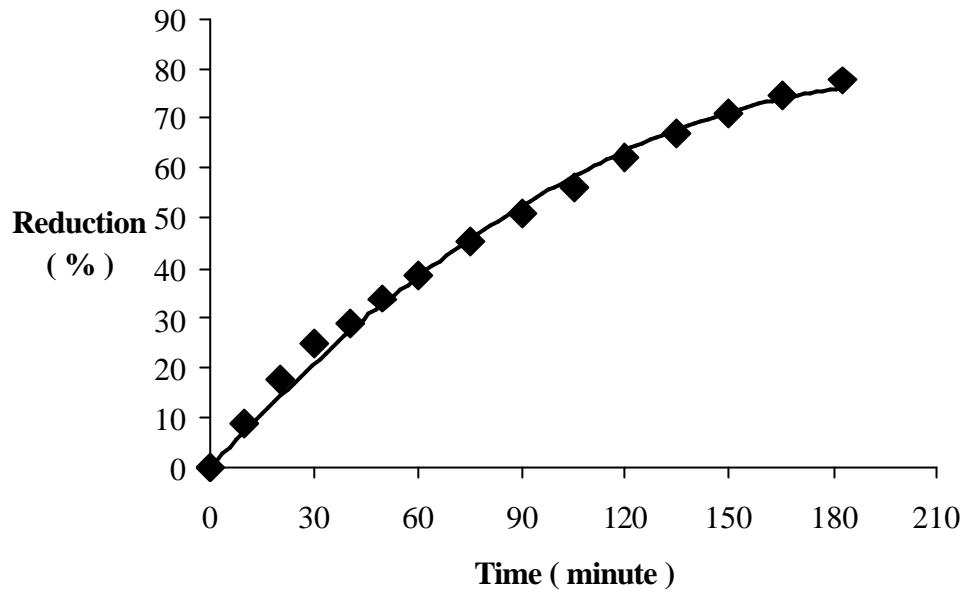


Figure 4.2 Reducibility Curve of Erdemir Sinter

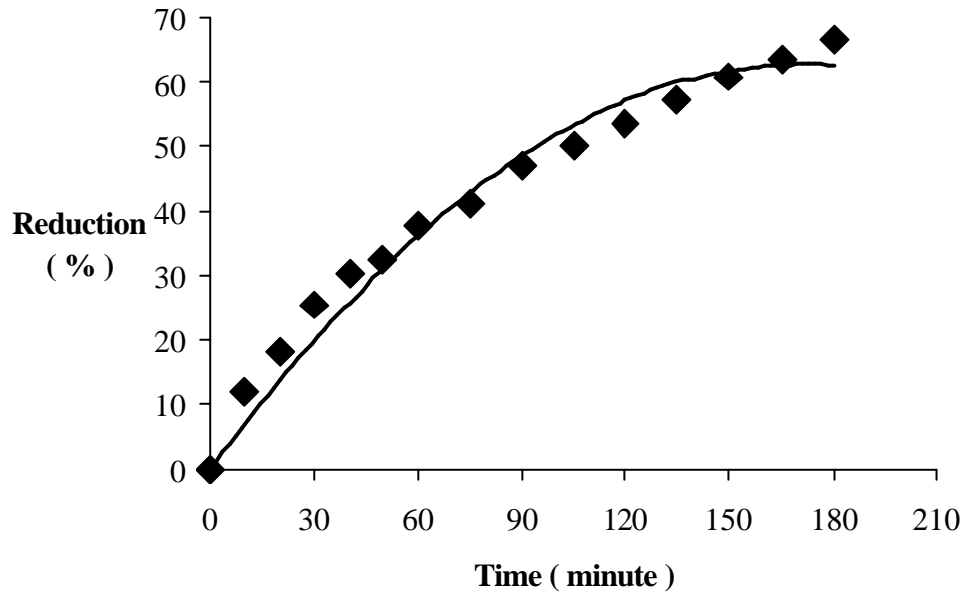


Figure 4.3 Reducibility Curve of Erdemir Pellet A

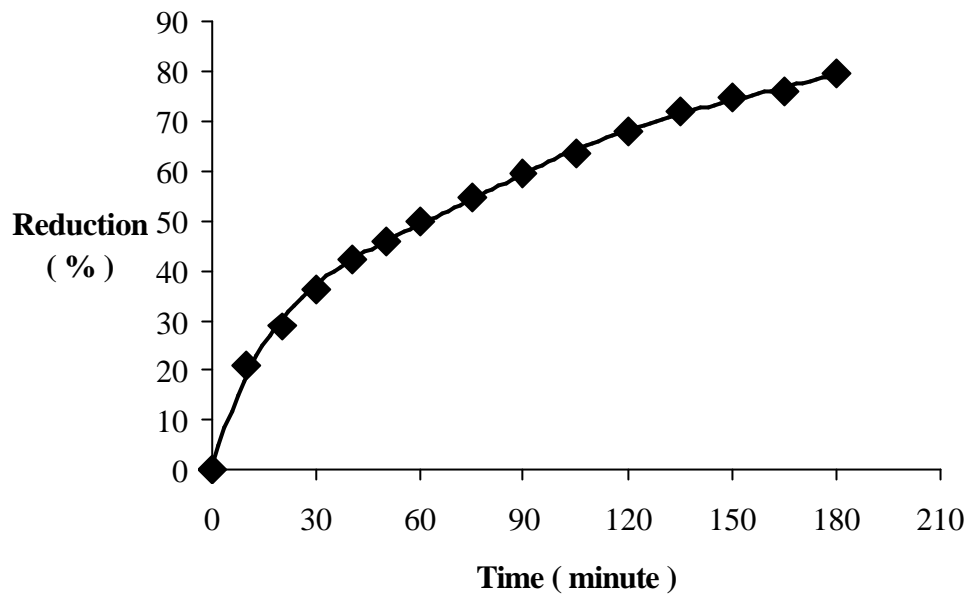


Figure 4.4 Reducibility Curve of Erdemir Pellet B

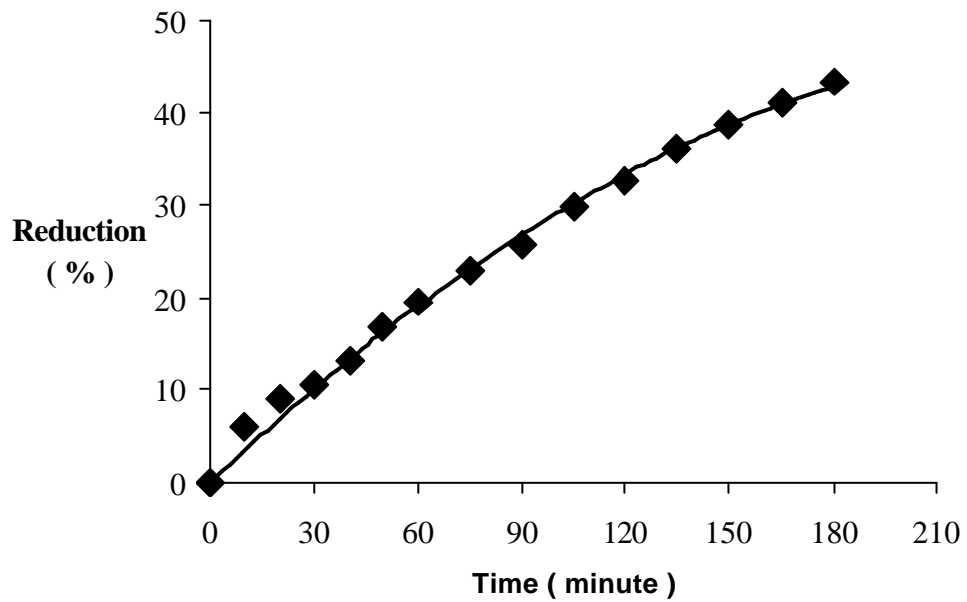


Figure 4.5 Reducibility Curve of Erdemir Lump Ore

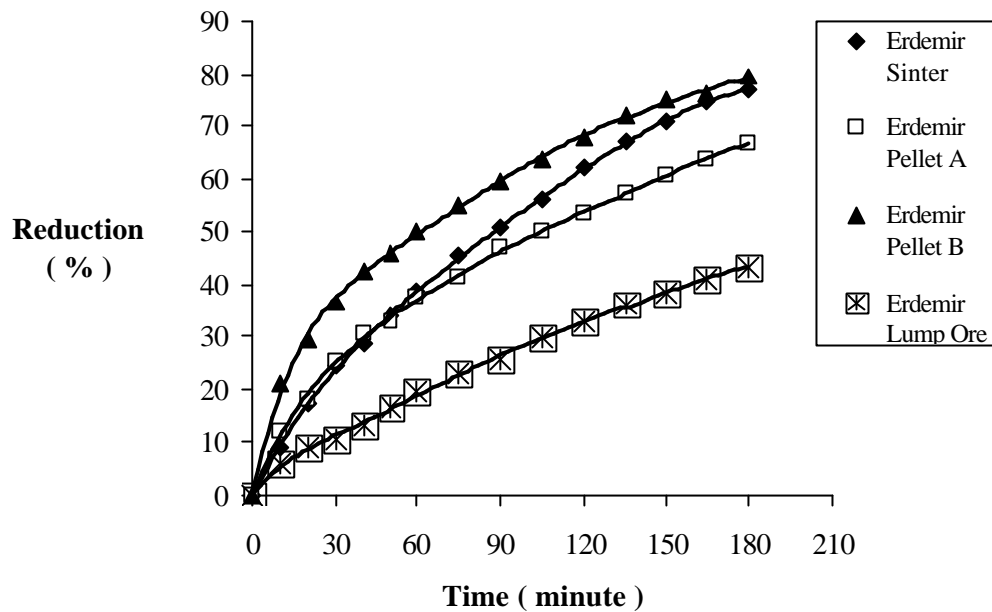


Figure 4.6 Comparison of Reducibilities of Erdemir Samples

#### 4.5 Evaluation of the Reducibility and Other Test Results

As it can be seen from Figure 4.6, among the Erdemir samples pellet B had the highest reducibility. This was most probably due to presence of high porosity in this blast furnace charge material. On the other hand, the reducibilities of Erdemir sinter, pellet A and lump ore decreased in the respective order. There was also a decrease in the porosities of these materials in the given order as seen from Table 4.3. So, there was one to one correspondence between the reducibilities measured and the porosities determined. On the contrary, Erdemir pellet B had the highest  $RDI_{0.5}$  value, which meant that it would form dust more than the other iron containing charge materials during handling. Most of Erdemir samples contained hematite as the major iron mineral. This mineral is known to be more easily reducible than magnetite. The chemical analysis of Erdemir samples indicated that they were in the acceptable ranges. The reducibility indices, k values, of Erdemir samples were quite high indicating good reducibilities especially for the pellets and the sinter.

When all of the local and imported lump iron ores were compared, as seen from Figure 4.7 that Koruyeri, Attepe and Hekimhan lump iron ores had the best reducibility. These ores were very porous as indicated in Table 4.3 and had easily reducible iron minerals such as hematite, goethite and limonite as summarized in Table 4.1. Among the lump ores of reasonable reducibility were Akdag, CVRD, Divrigi B Kafa and Dumluca. On the other hand, Divrigi Concentrate, Erdemir, ISCOR and Kesikköprü lump iron ores were difficult to reduce since some of them were high in magnetite content and had compact structure. So their calculated k values were quite low, as seen from Table 4.6. Among the lump iron ores, Divrigi Dumluca had the highest  $RDI_{0.5}$  value of 13.39%. It is observed from Table 4.3 that iron ores, containing limonite, goethite and having high porosity, had low densities. On the other hand, others, containing magnetite, hematite and having compact structure (low porosity), had higher densities.

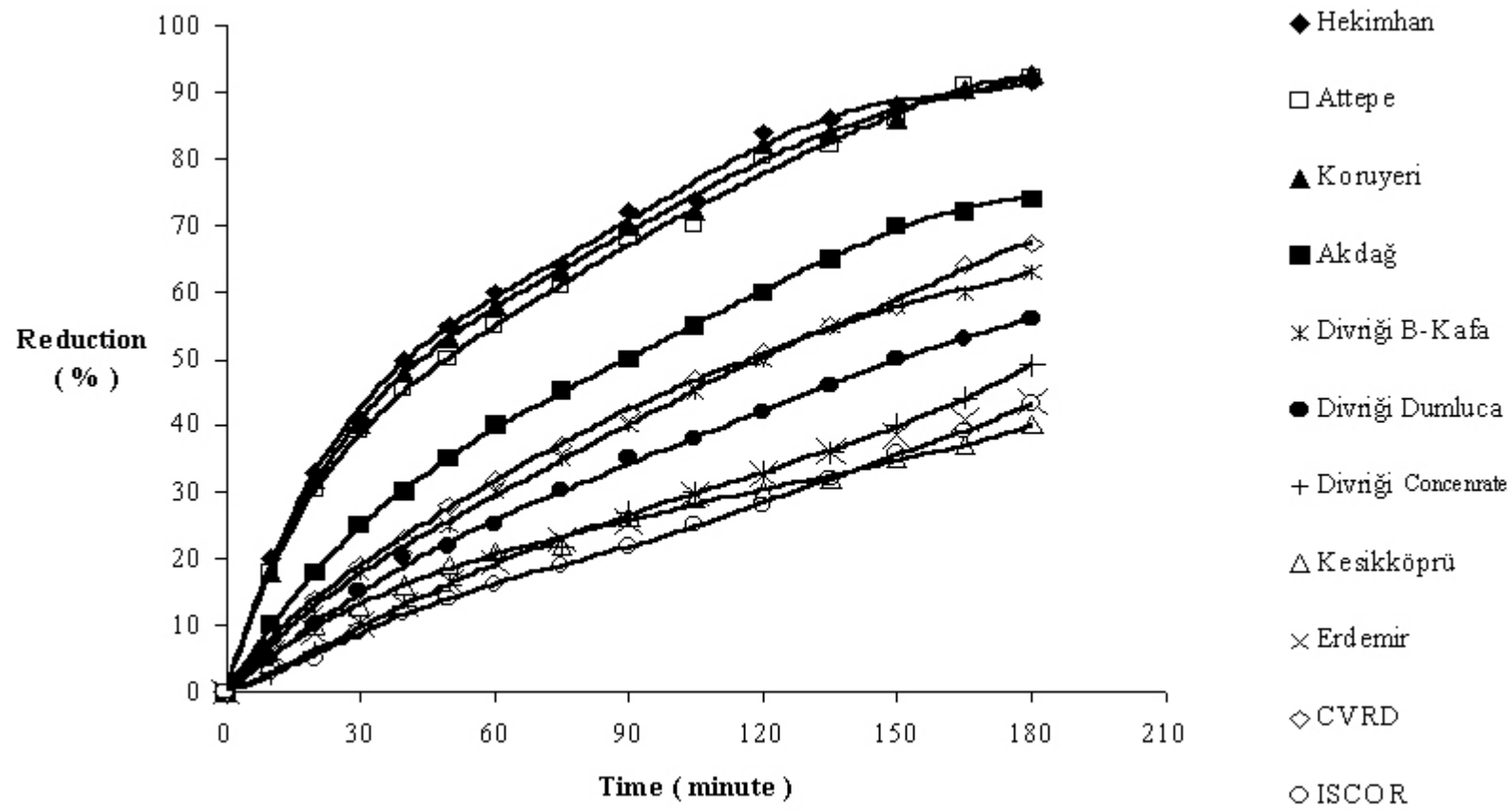


Figure 4.7 Comparison of Reducibilities Lump Ores [38,41,42]

When reducibility of the two kinds of imported pellets used at Erdemir and Divriği pellet produced locally were compared as seen in Figure 4.8, Erdemir pellet B was better than others. All the pellets tested contained hematite as the major iron mineral. Pellet B and Divriği pellet were more porous than pellet A. On the other hand, the dust index of pellet B was higher than those of Divriği pellet and Pellet A.

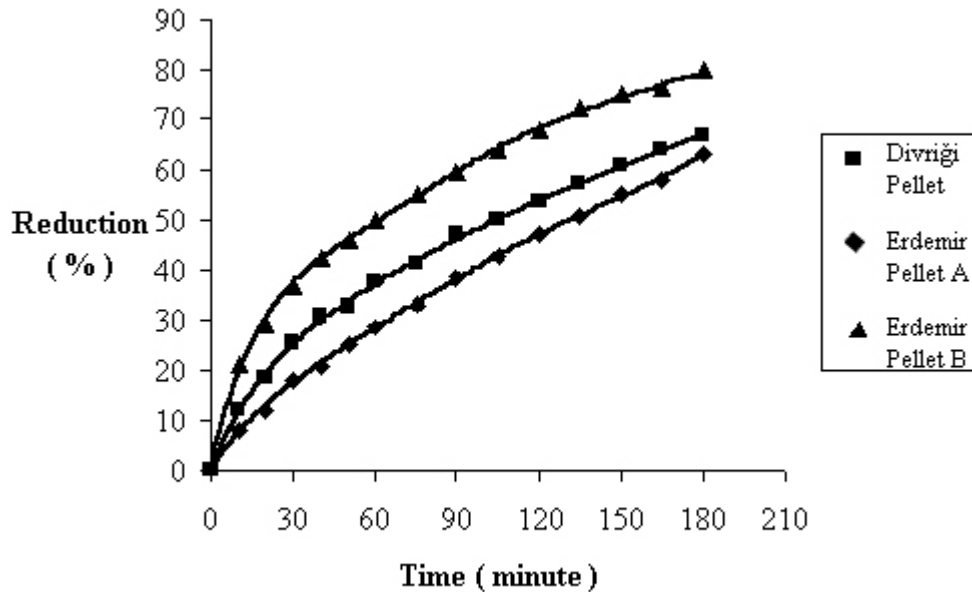


Figure 4.8 Comparison of Reducibilities of Pellets [38]

Finally, the comparison of the two different sinters produced at Erdemir and Kardemir showed that Erdemir sinter had slightly higher reducibility than Kardemir sinter as seen from Figure 4.9. Both sinters contained wustite, hematite and magnetite and had similar porosities. Although both values were acceptable, the dust index of Erdemir sinter was 5.36% whereas that of Kardemir was 3.62%. The reducibility index, e.g., k value of Erdemir was also higher than that of Kardemir.

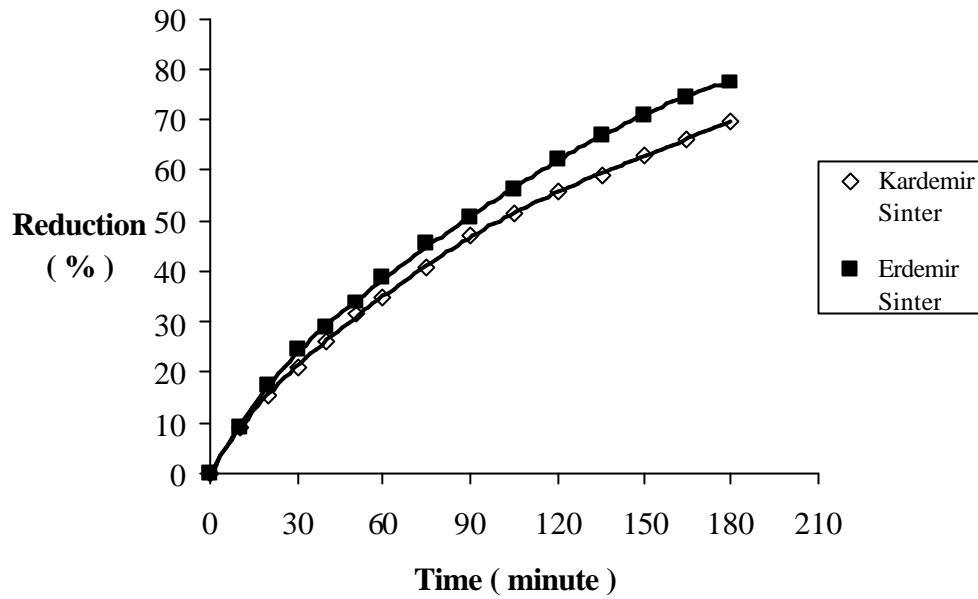


Figure 4.9 Comparison of Reducibilities of Sinters [39]

From the screen analysis done in the past [38], it was seen that none of the iron ores had particles greater than 40 mm and they had trace amount of particles greater than 30 mm. In the blast furnace, particles smaller than 5 mm cause serious problems. From this point of view, Divrigi Concentrate and Kesikköprü iron ore should have no problem in the blast furnace due to their low content of particles which were smaller than 5 mm. However, Akdag iron ore had a content of 10.55 % and Koruyeri iron ore had a content of 7.65 % of particles smaller than 5 mm. So, these ores would be expected to affect the blast furnace negatively. In Japan, percentage of particles which are greater than 30 mm is set to zero and percentage of particles which are smaller than 5 mm is limited between 2 and 3 %. When these limitations are satisfied;

- the gas use and distribution in the blast furnace will be more effective
- indirect reduction will increase
- coke consumption will decrease

Therefore, the efficiency of blast furnace will increase.

Such limitations in the size of charge will also result in;

- homogeneous distribution of the charge in the blast furnace.
- increase in the gas penetration of blast furnace.

As a result, the production improves.

Within certain limits, when the mean size of ore particle is decreased;

- specific surface area increases.
- solid/gas contact surface increases.

Thus, the reducibility increases.

To improve the gas penetration of blast furnace, large ore size is desired. However, for better reducibility, small sized ore and large specific surface area are desired. To optimize these conditions, generally, the higher limit of the ore size will be 25-50 mm and lower limit will be 5-10 mm. For the ores having a compact structure, the higher limit is generally 25 mm.

Another important finding was that, the amount of pellets which were smaller than 6.3 mm (3 mesh) was very small [38]. In the case of equivalence of the diameters of the pellets, space between the pellets will be the maximum resulting in a decrease of the resistance in the blast furnace against the gas flow. Thus, efficiency of blast furnace increases.

It should also be mentioned that RDI<sub>0.5</sub> (amount of particles smaller than 0.5 mm) is an important index for iron ores and other charge materials. A high value



of RDI  $_{-0.5}$  indicates that ore can be easily broken into pieces at low temperatures during reduction. This dust formation alters the distribution of the particle size of the feed of blast furnace.

A high value of RDI  $_{-0.5}$  ;

- decreases the gas penetration of blast furnace.
- increases loss of the charge material (in the dust form) as stack gas.

And also, a high value of RDI  $_{-0.5}$  affects the flow of gas adversely. So that, a low value of RDI  $_{-0.5}$  is desired.

So some properties expected from the blast furnace charge are;

- abrasion resistance,
- resistance against dust formation during transportation,
- ability to carry load in the blast furnace.

Erdemir specimens and the others had RDI values within the limitations as seen in Table 4.4. And also, these eleven different types of iron ores, two kinds of pellets and two kinds of sinters had the values which were closer to the upper limits. This indicated that, these iron ores, pellets and sinters had strong structures. Although a low reduction-degradation breakdown index RDI  $_{+3.35}$ , after reduction is considered bad for blast furnace operation, the limiting level is debatable. However, plant practice has shown that levels below 55-60% are undesirable. The values found for all the samples tested were higher than 80% so they could easily be accepted as good values.

Divrigi Concentrate, Divrigi pellet, and ISCOR iron ores had higher abrasion resistance and lower dust formation index with respect to Divrigi Dumluca, Attepe, Koruyeri iron ores, containing more hematite, limonite and goethite minerals.

#### 4.6 Models for Reduction

In order to obtain a satisfactory explanation for the observable kinetics of process a suitable model must be used. A number of models have been proposed for non-catalytic gas-solid reactions which include the reduction of iron ore [40]. Basically, all of these models are modifications of two extreme cases: the retracting core model and the homogeneous (or uniform reaction model). Which model will more closely represent the true situation depends on a number of factors and one of the criteria depends upon the porosity of the solid reactant. If the particles are sufficiently dense with little porosity, then a reaction interface will tend to form between unreacted and reacted solid, giving rise to the retracting core model in which the reaction interface progresses from the outside of the particle to the center during the course of the reaction. At the opposite extreme, if the particle is sufficiently porous, then the reacting gases can penetrate throughout the particle prior to reaction, so that when reaction occurs it is uniform throughout the particle, modified only by any pore diffusional gradients.

##### 4.6.1 Retracting Core Model

In reduction of small iron ore particles where intrinsic diffusion effects are negligible, it is realistic to assume that the overall reaction mechanism is controlled by the iron/wüstite interface. Since the reaction has been shown to be of first order then the rate of the reaction may be written as :

$$\frac{dN_n}{dt} = k'_A \left[ C_{Ai} - \frac{C_{Bi}}{K_e} \right] \quad \text{Eq.4.24}$$

where  $C_{Ai}$  and  $C_{Bi}$  are the respective interface concentrations of CO and CO<sub>2</sub>, and  $dN_n / dt$  is the net rate of reaction. If small particles and high flow rates are employed then it is reasonable to assume that the concentrations of A (CO or H<sub>2</sub>) and B (CO<sub>2</sub> or H<sub>2</sub>O) are the same at the interface and in the bulk gas. Thus, Eq.4.24 may be written as :

$$\frac{dN_n}{dt} = k'_A \left[ C_{Ab} - \frac{C_{Bb}}{K_e} \right] \quad \text{Eq.4.25}$$

where the subscript b refers to bulk concentrations.

If the retracting core model is applicable and a pseudo-steady for the material balance is assumed, then Eq.4.25 may be expressed in terms of the shrinkage of the core.

$$-\frac{dN_0}{dt} = -\frac{dN_n}{dt} = -C_0 \frac{dV}{dt} = -C_0 \frac{d}{dt} \left( \frac{4}{3} \pi r_i^3 \right) \quad \text{Eq.4.26}$$

where  $C_0$  is the atomic density of oxygen in the ore,  $r_i$  is the core radius and  $dN_0 / dt$  is the rate of oxygen removal.

Based on the unit area of the unreacted core we have from Eq.4.26 ;

$$-\frac{1}{4\pi r_i^2} \frac{dN_0}{dt} = -\frac{1}{4\pi r_i^2} \frac{dN_n}{dt} = -\frac{C_0}{4\pi r_i^2} 4\pi r_i^2 \frac{dr}{dt} \quad \text{Eq.4.27}$$

and on equating Eq.4.25 and Eq.4.27 and integrating between  $r = r_0$  at  $t = 0$  and  $r = r_i$  at  $t = t$

$$1 - \frac{r_i}{r_0} = \frac{k'_A}{C_0} \left( C_{Ab} - \frac{C_{Bb}}{K_e} \right) t \quad \text{Eq.4.28}$$

$t = 0$  and in terms of fractional reduction  $R$ ;

$$\left[1 - (1 - R)^{1/3}\right] = \frac{k'_A}{r_0 C_0} \left( C_{Ab} - \frac{C_{Bb}}{K_e} \right) \quad \text{Eq.4.29}$$

Thus, if the reaction was interface controlled a plot of  $[1 - (1 - R\% / 100)^{1/3}]$  against time should yield a straight line.

$[1 - (1 - R\% / 100)^{1/3}]$  versus time plot was drawn for the reduction of Erdemir samples but a straight line could not be obtained.

#### 4.6.2 Porous Solid Model

For the case of almost uniform gas penetration within the pores of the particle, internal reduction predominates and the rate is controlled primarily by gas – solid reaction on the pore walls. The model assumes that after the formation of a thin layer and its diffusion is rapid so that the reaction rate is determined by reaction of  $H_2$  (or  $CO$ ) with the oxide. If the reaction is assumed to take place uniformly throughout the whole particle then the rate of reaction can be written as;

$$\frac{dW_r}{dt} = -W_r S k'_A (C_{Ab} - C_{Ae}) \quad \text{Eq.4.30}$$

where  $W_r$  is the amount of oxygen in the sample at time  $t$ ,  $S$  is the usable pore surface area of wüstite per unit mass of oxygen and the other quantities have their usual meaning.

Eq.4.30 can be written in terms of the fractional reduction  $R$  as;

$$R = \frac{W_0 - W_r}{W_0} = 1 - \frac{W_r}{W_0} \text{ or } \frac{W_r}{W_0} = 1 - R \quad \text{Eq.4.31}$$

where  $W_0$  is the initial weight of oxygen in the sample. Substituting Eq.4.31 in Eq.4.30 and integrating we get;

$$\ln(1 - R) = -Sk'_A (C_{Ab} - C_{Ae})t \quad \text{Eq.4.32}$$

Thus, a plot of  $[-\ln(1-R)]$  against time should give a straight line if this mechanism is obeyed.

The reducibility index values,  $k$ , obtained from the slope of graph of  $[-\ln(1-R\%/100)]$  versus time which are plotted in Figures 4.10 to 4.13, are presented in Table 4.6.

Table 4.6 Reducibility Indices of Erdemir Samples and the Others

Sample	Reducibility index, $k, \text{hour}^{-1}$
<i>Erdemir Lump Ore</i>	0.2
<i>Erdemir Pellet A</i>	0.38
<i>Erdemir Pellet B</i>	0.56
<i>Erdemir Sinter</i>	0.49
<i>Kesikköprü</i>	0.12
<i>Divrigi Concentrate</i>	0.23
<i>Divrigi (Dumluca)</i>	0.25
<i>Divrigi B-Kafa</i>	0.32
<i>Divrigi Pellet</i>	0.36
<i>Akdag</i>	0.4
<i>Attepe</i>	0.65
<i>Koruyeri</i>	0.69
<i>Hekimhan</i>	0.72
<i>Kardemir Sinter</i>	0.41
<i>CVRD</i>	0.34
<i>ISCOR</i>	0.19

As seen from the figures,  $[-\ln(1 - R\% / 100)]$  versus time graphs were linear. So that, the reduction mechanism of Erdemir samples obeyed the porous solid model.

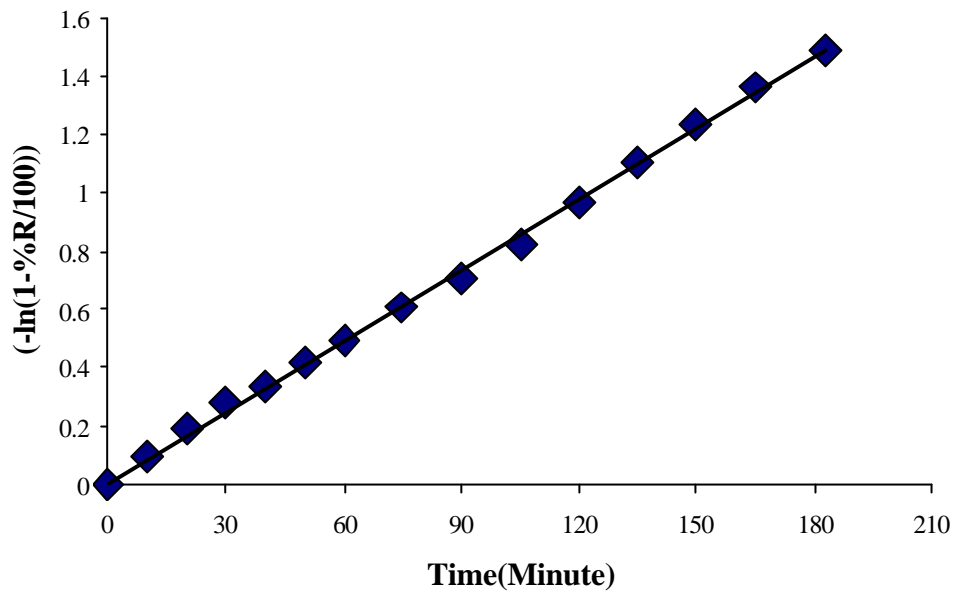


Figure 4.10  $[-\ln(1 - R\% / 100)]$  vs Time (t) Graph to Determine the Reducibility Index for Erdemir Sinter

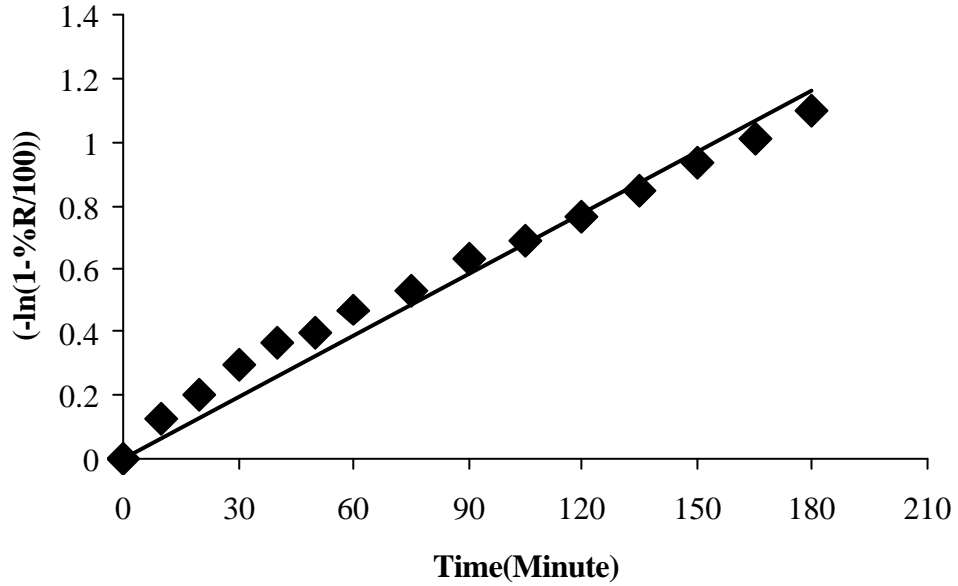


Figure 4.11  $[-\ln(1 - R\% / 100)]$  vs Time (t) Graph to Determine the Reducibility Index for Erdemir Pellet A

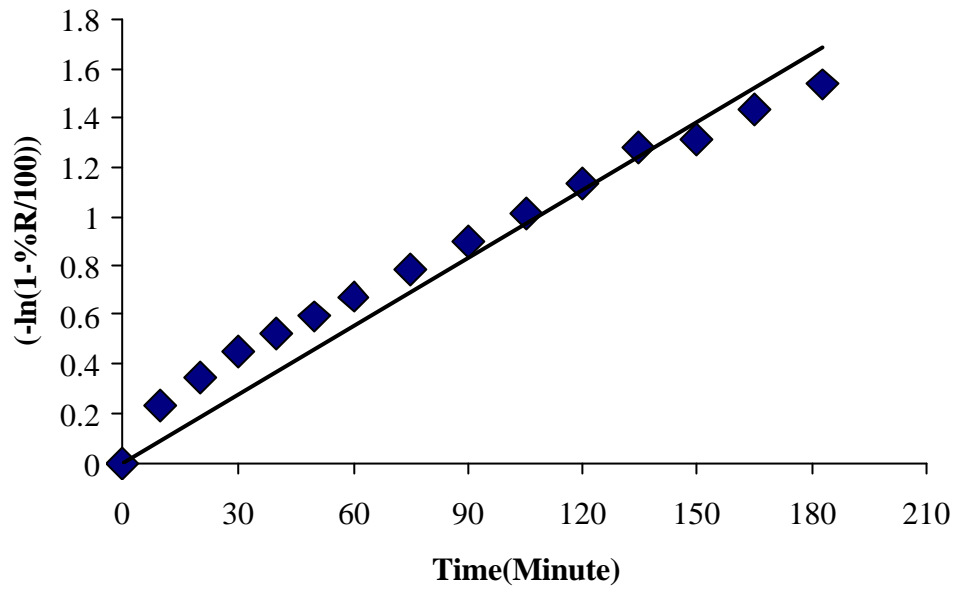


Figure 4.12  $[-\ln(1- R\% / 100)]$  vs Time (t) Graph to Determine the Reducibility Index for Erdemir Pellet B

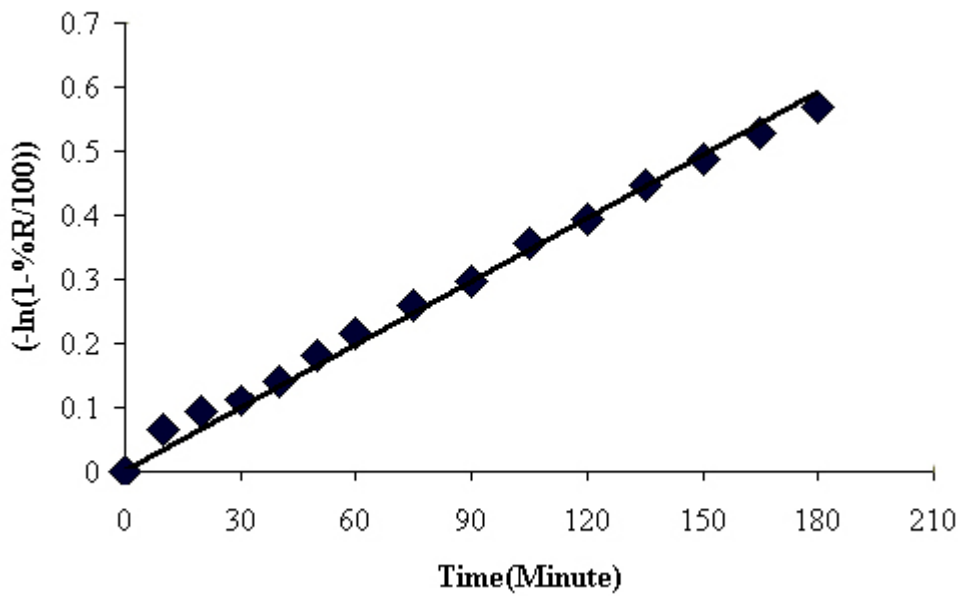


Figure 4.13  $[-\ln(1- R\% / 100)]$  vs Time (t) Graph to Determine the Reducibility Index for Erdemir Lump Ore

## CHAPTER 5

### CONCLUSIONS

The aim of this study was to investigate the behaviour of Erdemir samples under certain conditions and to investigate how the reducibility changes according to certain properties. For this study, Erdemir lump ore, Erdemir pellets (A, B) and Erdemir sinter were investigated.

Samples, having the size range of 10–12.5 mm, were subjected to mineralogical inspections by the help of X-ray diffraction patterns. Erdemir samples were mainly composed of hematite ( $\text{Fe}_2\text{O}_3$ ). Erdemir sinter was mainly composed of hematite ( $\text{Fe}_2\text{O}_3$ ), magnetite ( $\text{Fe}_3\text{O}_4$ ), wustite ( $\text{FeO}$ ), calcium ferrite ( $\text{CaFe}_5\text{O}_7$ ) and dicalcium silicate ( $2\text{CaO}\cdot\text{SiO}_2$ ).

Porosity is an important parameter for strength and reducibility properties of a blast furnace burden. In order to calculate the porosities of Erdemir samples, first true density values were measured with water pycnometer. After that, apparent density values were measured with mercury pycnometer. The difference between true density and apparent density values was calculated in percentage as the total porosity values. Erdemir pellet (B) had the highest porosity value of 33.5 %, and lump ore had the lowest value of 8.1 %, among the samples.

Reduction disintegration indices of the samples were measured which gave degradation tendency of the burden during transferring from stack to bottom portions of the blast furnace. Samples, subjected to reduction disintegration tests, were reduced at 550 °C and cooled to room temperature. Afterwards, samples



were revolved in a tumbler drum with a 30 rev./min. for 30 minutes. They were later screened with appropriate screens. The weights of +6.7 mm, -6.7 mm + 3.35 mm and -3.35 mm +500  $\mu$ m sized particles were determined. Erdemir samples had enough strength and reasonably low dust formations.

The reducibility values of Erdemir samples were determined by Gakushin tests. Samples were subjected to reduction at 900 °C by using carbon monoxide (CO) and nitrogen (N<sub>2</sub>) gases. Reducibility data were collected for 3 hours. Erdemir lump ore had the lowest reducibility value of 43.4 % among the samples and Erdemir pellet (B) had the highest reducibility value of 78.7 %. The main reason for this difference was due to porosity since porous structures provide more surface area to contact with the reducing gas, which make the reduction easy. Reduction kinetics of Erdemir samples were also investigated. It was observed that the reduction mechanism obeyed the porous solid model.

As a future study, it is recommended that the reducibility and reduction degradation tests should be done by using the recently accepted ISO standards. But for this purpose, it is necessary to purchase or set-up equipment that satisfy the ISO standards.

## REFERENCES

- 1) D. F. Ball, Agglomeration of Iron Ores, American Elsevier Pub. Co., (1973), p.52-58
- 2) Economic Aspects of Iron Ore Preparation, United Nations (1966), p.7
- 3) Clarke, F.W., and Washington, H.S., The Composition of the Earth's Crust, U.S. Geol.Surv., (1924), Prof.. Paper 127
- 4) Merklin, K.E., and Vaney, F.D., The Coarse Specalurite-Fine Magnetite Pelletizing Process, Agglomeration, Interscience Publishers, (1962), p.965
- 5) Linder, R., Programme Controlled Reduction Test for Blast Furnace Burdens, J. Iron Steel Institute, London, July (1958), p.233
- 6) Holowaty, M.O., and Squarcy, C.M., High Temperature Testing of Blast Furnace Coke, AIME Blast Furnace, Coke Oven and Raw Materials Conference, April (1957)
- 7) Cohen, E., Radiographic Studies of the Process of Sintering Iron Ores , J. Iron and Steel Institute, (1953), 175, p.160- 166
- 8) Wild, R., The Chemical Constitution of Sintors, J. Iron and Steel Institute, (1953), 174, p.131-135

- 9) Moleva, N. G., and Kusakin, P.S., Mineralogical Make-Up of Fluxed Sinters, *Stal*, (1957), 17, p.1068-1071; Henry Brutcher Translation No. 4142
- 10) Knepper, W.A., Snow, R.B., and Johnson, R.T., Study of the Properties of Self-Fluxing Sinters, Agglomeration, Interscience Publishers, New York, (1962), p.787-804
- 11) Kissin, D.A., and Litvinova, T.I., Mechanism of Mineral Formation in Sintering Fluxed Sinter, *Stal* (in English), (1960), No. 5, p.318-323
- 12) ASTM: Drop Shatter Test for Coke, D141-48. ASTM Standards, (1949), 5, p.672-676
- 13) Joseph, T.L., Barrett, E.P., and Wood, C.E., Iron Oxide Sinters, Composition, and Deoxidation, *Blast-Furnace and Steel Plant*, (1933), 21, p.147-150 , 207-210 , 260-263 , 321-323 , 336
- 14) Hamilton, F.M., and Ameen, H.E., Physical Tests and Results of Some Agglomerated Iron Ores, Blast-Furnace, Coke Oven, and Raw Materials Proceedings, AIME, (1951), 10, p.135-140; Laboratory Studies on Iron Ore Sintering and Testing, Transactions, AIME, (1950), 187, p.1275-1282
- 15) Morrissey, H.A., Impact Test on Sinter and Its Applicability to Quality Control, Special Report No. 278B-4, Mellon Institute of Industrial Research, Pittsburgh, Pennsylvania, February, (1953)
- 16) Holowaty, M.O., Goldfein, H.A., and Sheets, C.B., Study of the Productivity of Conventional Dwight-Lloyd Sintering Machine, Blast-Furnace, Coke Oven and Raw Materials Proceedings, AIME, (1955), 14, p.43-75
- 17) Powers, R.E., Tumble Test on Sinter, Special Report No.278B-3, Mellon Institute of Industrial Research, Pittsburgh, Pennsylvania, April 16, (1952)

- 18) Dartnell, J., JISI , (1969), 207, p.282-292
- 19) Callender, W., Agglomeration, Interscience, New York, (1962), p.647-667
- 20) Kister, H., Stahl und Eisen, (1968), 88, p.1427-1428
- 21) Oliver, R.A., JISI ,(1967), 205, p.1131-1135
- 22) Kikuchi, T., JISI , (1967), 205, p.606-624
- 23) Bogdandy, L.V., Dickens, P., Esche, W.V., and Willems, J., 3rd Jornees International de Siderurgie, October, (1962). Luxembourg , p.142-156 (BISIT 3033)
- 24) Poos, A., and Linder, R., 3rd Jornees International de Siderurgie, October, (1962). Luxembourg , p.117-126 (BISIT 3032)
- 25) Berg, B., Hancart, J., and Poos, A., Rev. Universelle Mines, (1962), 18 , p.284-287
- 26) Dickens, P., Esche, W.V., and Willems, J., Stahl und Eisen, (1959), 79, p.905-917
- 27) I.S.O. 4695, Iron Ores – Determination of Reducibility, I.S.O. Standard, (1995 and 1996)
- 28) I.S.O. 4696-1, Static Test for Low Temperature Reduction-Disintegration, I.S.O. Standard, (1996)
- 29) I.S.O. 4696-2, Static Test for Low Temperature Reduction-Disintegration, I.S.O. Standard, (1998)

- 30) I.S.O. 4697, Iron Ores – Test Method for Low Temperature Disintegration – Tumbling during Reduction, I.S.O. Standard, (1990)
- 31) I.S.O. 7215, Iron Ores – Determination of Relative Reducibility, I.S.O. Standard, (1995)
- 32) I.S.O. 7992, Iron Ores – Determination of Reduction Properties under load, I.S.O. Standard, (1992)
- 33) I.S.O. 13930, Iron Ores – Dynamic Test for Low Temperature Reduction Disintegration, I.S.O. Standard, (1998)
- 34) Poos, A., CNRM Met. Report No.19 , June (1969), p. 39
- 35) JIS 8713, Determination of Iron Ores Reducibility, Japanese Standard , (1967)
- 36) TS 4400, Determination of True Density of Ceramic and Refractory Materials by Pycnometer, Turkish Standards Institute, (1985)
- 37) TS 4379, Determination of Apparent Density of Granular Ceramic and Granular Refractory Materials – Mercury Displacement Method, (1985)
- 38) Sevinç, N., Topkaya, Y., Geveci, A., and Timuçin, M., Determination of Physical, Chemical, Mineralogical and Reduction Properties of Some Lump Iron Ores and Divrigi Pellet, used at Isdemir, Project Report, Metallurgical and Materials Engineering Department, Middle East Technical University, Ankara (1987)
- 39) Günaydin A., Disintegration Indices of Steelmaking Slag Added Iron Ore Sinters (Thesis submitted to the Graduate School of Natural and Applied Sciences of the Middle East Technical University), May 2002

40) Hughes, R., The Reduction of Iron Ores by  $H_2$  and CO and Their Mixtures, Thermochemica Acta, (1982) , Vol. 59, p.361-372

41) Topkaya, Y., Geveci, A., and Aydogdu, A., Determination of Reduction Properties of CVRD Iron Ore, used at Isdemir, Project Report, Metallurgical and Materials Engineering Department, Middle East Technical University, Ankara (1991)

42) Topkaya, Y., Geveci, A., and Aydogdu, A., Determination of Reduction Properties of Iscor and Attepe Ores, used at Isdemir, Project Report, Metallurgical and Materials Engineering Department, Middle East Technical University, Ankara (1991)